Abstract

Reasonably homogeneous, polycrystalline, n-type InSb-GaSb semiconducting alloys have been produced by the directional freezing technique. This material has been used to measure the Hall coefficient and the conductivity as a function of the temperature and composition. Values of the extrapolated thermal energy gap and of the mobility temperature exponent have been obtained for specimens covering the composition range between 70 and 94 mol % GaSb.

The occurrence of two energy gaps for GaSb has been explained by means of a three carrier analysis of the electrical results taken from the literature. The result of this analysis has been used with some other known experimental and theoretical results in order to explain the variation of the energy gap of the InSb-GaSb alloys as a function of composition.

The InAs-In_2SeTe alloy system was investigated: the limit of solid solution was determined by X-ray techniques, the Hall coefficient and the optical energy gap were measured as a function of composition. The height of the second lowest conduction band above the valence band for InAs and the maximum electron concentration required to fill the (000) minimum up to the lowest level of the ⟨111⟩ minima were obtained.

Acknowledgements

I should like to thank Dr. J.C. Woolley for suggesting this problem and for his advice throughout. I have benefited from his great competence in the field of alloy semiconductors. I also wish to express my appreciation to all the technicians of the physics department for building some of the apparatus and to Mr. Lavallée for tracing the graphs and diagrams.

Table of Contents

Chapter 4
The InAs-In_2SnTe Cross-Substitutional Alloy System

Appendix

List of Illustrations

Chapter 1

Introduction

1.1. Band structure of alloy semiconductors.

Semiconductor alloys are crystalline solids whose atomic structure is characterized by a substantial degree of disorder. The disorder results from the essentially random arrangement of the solute atoms among the available ordered lattice sites.

In a perfect crystal, the electronic energy levels fall into well-defined bands. The extension of the band theory to disordered crystals has been carried out by means of the perturbation theory (1). The potential acting on an electron moving through a disordered alloy is decomposed as follows:

$$V_{alloy}(r) = V_{periodic}(r) + V_{non\text{-}periodic}(r)$$

where $V_{periodic}(r)$ is the average of the alloy potential over all possible random configurations of atoms in the alloy and $V_{non\text{-}periodic}(r)$ the deviation of $V_{alloy}(r)$ from its average, $V_{periodic}(r)$. The "virtual crystal" is defined by the periodic component $V_{periodic}(r)$, and is adopted as the unperturbed system of the perturbation theory. The disorder potential $V_{non\text{-}periodic}(r)$ is regarded as the perturbing potential. In those cases where alloying is physically possible, the different atoms are sufficiently similar that $V_{non\text{-}periodic}$ has a relatively small value and hence normal perturbation theory can be applied. Then, the energy band structure of the alloy is determined by solving the Schrödinger wave equation

$$\nabla^2\psi + \frac{2m}{\hbar^2}\left[E - V_{periodic}(r)\right]\psi = 0.$$

It has been shown that the exact form of the energy surfaces within a Brillouin zone, and in particular the magnitude of the energy discontinuities across its boundaries, depend on the atomic concentration and degree of disorder within the alloy. On the other hand, the form and size of a zone depend on the crystal structure alone. The disorder has only a minor effect on the energy level distribution near the middle of an unperturbed band whereas, near the top or bottom it can have an important effect. The net effect is that band edges are smeared out into the forbidden bands. This smearing out is always finite in extent, particularly in the case mentioned above, so that the forbidden bands need not disappear altogether. In order to understand the properties of the alloys it has been proposed that a band picture similar to that of the compounds themselves is retained by the alloys, this being the band structure corresponding to the virtual crystal. Thus the alloy properties may be described by the same parameters as the compounds. This virtual crystal model of an alloy has been satisfactorily applied to several alloy systems. A detailed knowledge of the band structure of the separate components is a prerequisite to the successful exploration of the intermediate alloys, although in some cases data for the alloys has helped to clarify the band structure of the separate components.

1.2. Properties of InSb-GaSb semiconducting alloys.

So far, among the limited number of III-V semiconducting alloys which have been investigated, it was found that they are miscible in all proportions and have the same structure as the constituent compounds, namely the zinc-blende structure (2). In most of these alloy systems, the rate of diffusion is very slow and solid, homogeneous,

single phase specimens suitable for physical measurements, such as Hall effect and optical absorption, have usually been produced by the directional freezing technique. InSb-GaSb alloys have extensively been prepared by this method (3) and a great deal of work has been carried out to determine their electrical and optical properties. It is intended to outline in this section the work done on this alloy system prior to the present work described in this thesis.

The variation of lattice parameter as a function of composition in the InSb-GaSb system was reported by Woolley et al (4). They annealed compressed powder specimens at a temperature very close to the solidus curve for eight weeks. The proper temperature was found by trial and error since the solidus curve was not known. The progress towards equilibrium was followed by taking X-ray powder photographs. A single phase solid solution was found to occur at all compositions. A graph of the variation of the lattice parameter against composition is shown in Fig. 1. It is seen that the lattice parameter varies almost linearly with composition, therefore Vegard's law is probably obeyed within the limit of experimental error.

The complete phase diagram of the InSb-GaSb alloy system was reported by Woolley and Smith (3) and it is shown in Fig. 2. The form of the liquidus curve was obtained by normal cooling-curve techniques and the form of the solidus curve by heating-curve techniques and by an X-ray method. The same workers also showed that the tie lines in the liquidus-solidus region lie in the GaSb-InSb plan of the In-Ga-Sb ternary system. This indicates that the alloy system is pseudo-binary. Finally, the InSb-GaSb alloys have the same structure as the constituent compounds, namely the zinc-blende structure.

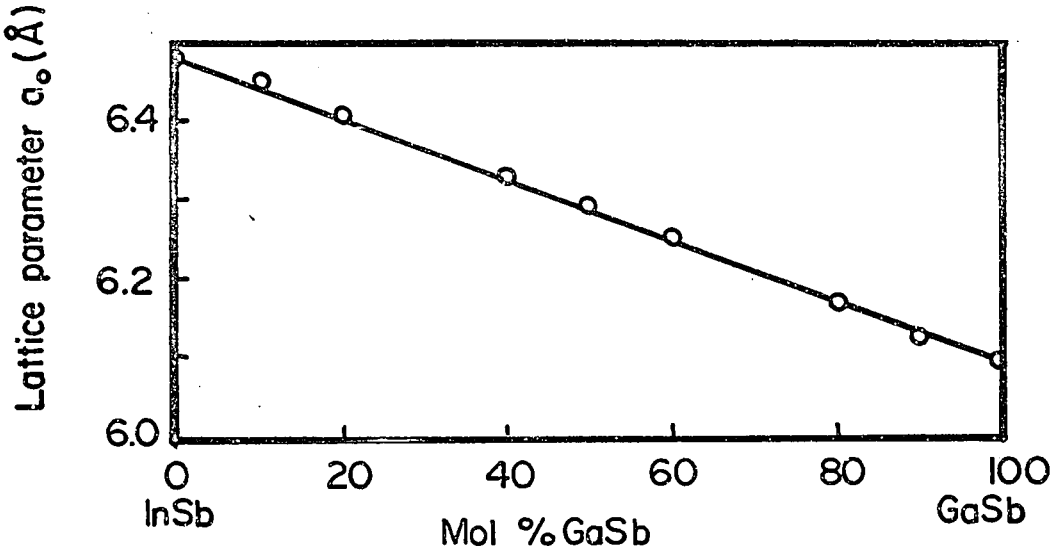

Fig. 1 Variation of lattice parameter a_o as a function of composition in the GaSb-InSb system.

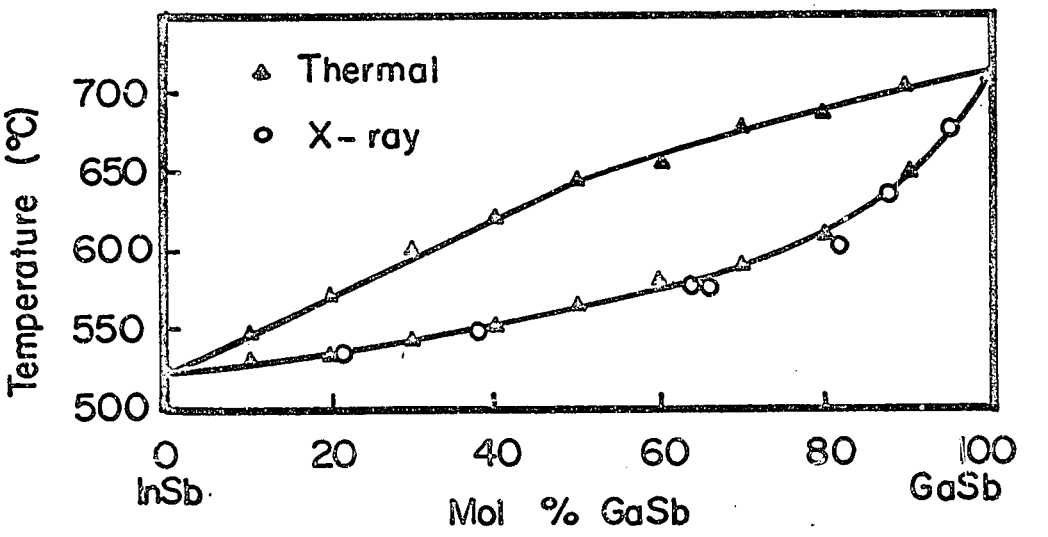

Fig. 2 Equilibrium diagram of GaSb-InSb system.

A great deal of work has been carried out to determine the electrical and optical properties of the InSb-GaSb alloy system. Optical absorption measurements have been reported by Woolley, Evans and Gillett (5) and by Woolley and Evans (6), and reflectivity measurements by Woolley and Blaney (7). The fundamental optical energy gap was found to change gradually but non-linearly from InSb to GaSb and also it was found to vary linearly with temperature. A sketch of the GaSb and InSb band structures is shown respectively in Figs. 3 and 4. The reflectivity peaks corresponding to the $X_5 \rightarrow X_1$ transition and to the $\Lambda_3 \rightarrow \Lambda_1$ transition showed a linear variation with composition which is consistent with a virtual crystal model. It should be noted, that the fundamental optical energy gap corresponds to vertical electronic transitions from the top of the valence band to the bottom of the conduction band in the (000) direction while the $X_5 \rightarrow X_1$ transition corresponds to vertical electronic transitions in the $\langle 100 \rangle$ directions and the $\Lambda_3 \rightarrow \Lambda_1$ transition to vertical electronic transitions to points at approximately $\langle 1/6, 1/6, 1/6 \rangle$ in k-space. This can easily be seen from a sketch of the GaSb band structure shown in Fig. 3. The fact that the optical energy gap does not vary linearly with composition indicates that the (000) conduction band minimum is sensitive to perturbations due to crystal potential variations and hence may show deviations from the virtual crystal predictions (8). The other regions of the conduction and valence bands are much less sensitive to perturbations.

The electrical properties of the InSb-GaSb alloy system have been reported by Woolley and Gillett (9). The thermal energy gap values for the alloys were determined from measurements of the

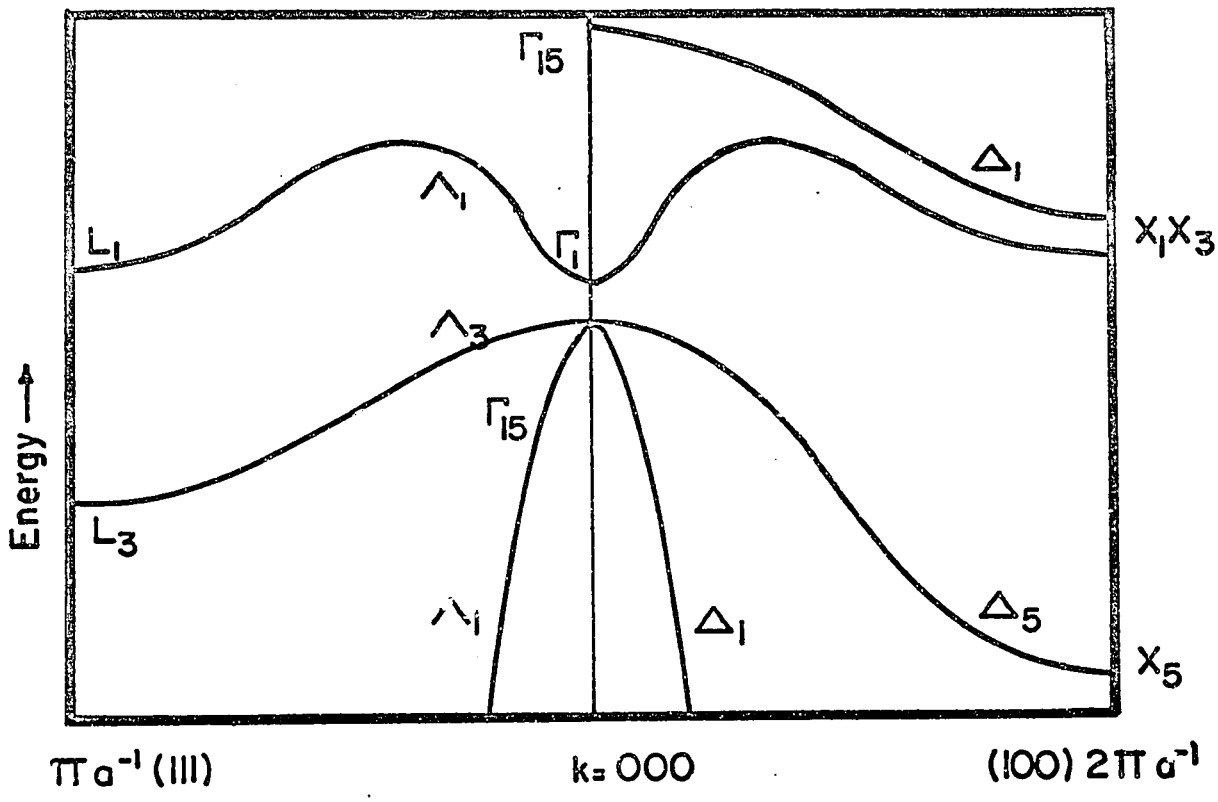

Fig. 3 Band structure of GaSb (after Ehrenreich).

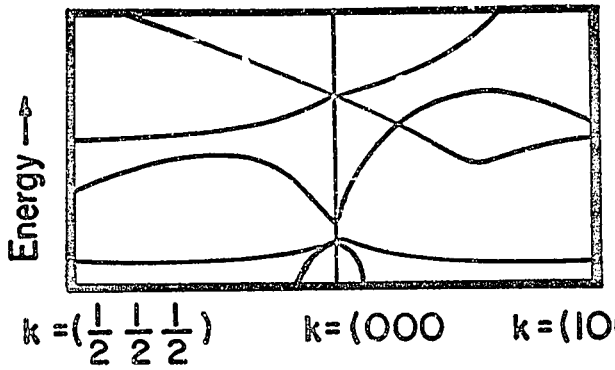

Fig. 4 Band structure of InSb (after Herman).

Hall coefficient as a function of temperature (90-850°K). In the composition range 20-100 mol % GaSb the specimens were p-type in the impurity region, and as the temperature was raised each showed a transition from p-type to n-type behaviour where intrinsic effects were observed. Thus, two-carrier formulae had to be used in the analysis of the Hall effect measurements. The number of electrons n and the number of holes p were determined from these formulae. It can be shown that the product np is given by the following equation (10):

$$\frac{np}{T^3} = A(m_n m_p)^{3/2} e^{-Eg/kT}$$

where A is a constant, m_n the effective electron mass, m_p the effective hole mass, k the Boltzmann's constant, T the absolute temperature and Eg the thermal energy gap. Now assuming that $Eg = E_o + \beta T$ in the temperature range considered, and that m_n and m_p are independent of T, the above equation can be written as

$$\log_{10}\frac{np}{T^3} = \log_{10}A + \frac{3}{2}\log_{10}(m_n m_p) - \frac{E_o}{2.303kT} + \frac{\beta}{2.303k}$$

Hence the slope of the graph $\log_{10} np/T^3$ against 1/T gives E_o the energy gap extrapolated to absolute zero. When these graphs were plotted for alloys covering the whole composition range, it was seen that, for alloys containing less than 65 mol % GaSb, a large part of each graph was linear in the intrinsic region, giving one unique value of the energy gap E_o. However, for alloys containing more than 65 mol % GaSb the graphs showed two distinct linear parts in the intrinsic region. Thus for these alloys two values of the energy gap

were obtained, a low temperature and a high temperature value, as well as a transition temperature T_c. The variations of the extrapolated thermal energy gap E_o and transition temperature T_c with composition is shown in Fig. 5. Also shown in Fig. 5 is the variation of the extrapolated optical energy gap as a function of composition. It is seen from these results that for compositions between 0 and 65 mol % GaSb the alloys behave in the normal way. The forbidden energy gap of InSb is progressively changed with the addition of GaSb and the values obtained from electrical and optical measurements are in good agreement. It thus appears that the band form of InSb with the conduction band minimum at (000) in k-space is retained by the alloys in this composition range. However, the results obtained for alloys in the composition range 65-100 mol % GaSb seem anomalous. It is seen from Fig. 3 that the lowest conduction band minimum of GaSb occurs at k = 000. Since the low temperature electrical energy gap is in agreement with the optical energy gap for GaSb and since the values of the optical energy gap show a monotonic variation from InSb to GaSb, it may be concluded that the optical absorption data show the variation of the energy gap at k = 000. It therefore appears that the electrical data show other conduction band minima which move below the conduction band minimum at k = 000 over the composition range 65-100 mol % GaSb. The low temperature electrical energy gap may then be attributed to an indirect transition not observed in the optical absorption measurements. Finally, the electrical data also show that there are probably other conduction band minima, their effect is only observed at high temperature. Thus it may be seen that the electrical measurements do not follow the normal variation as a function of temperature and composition as do the optical results.

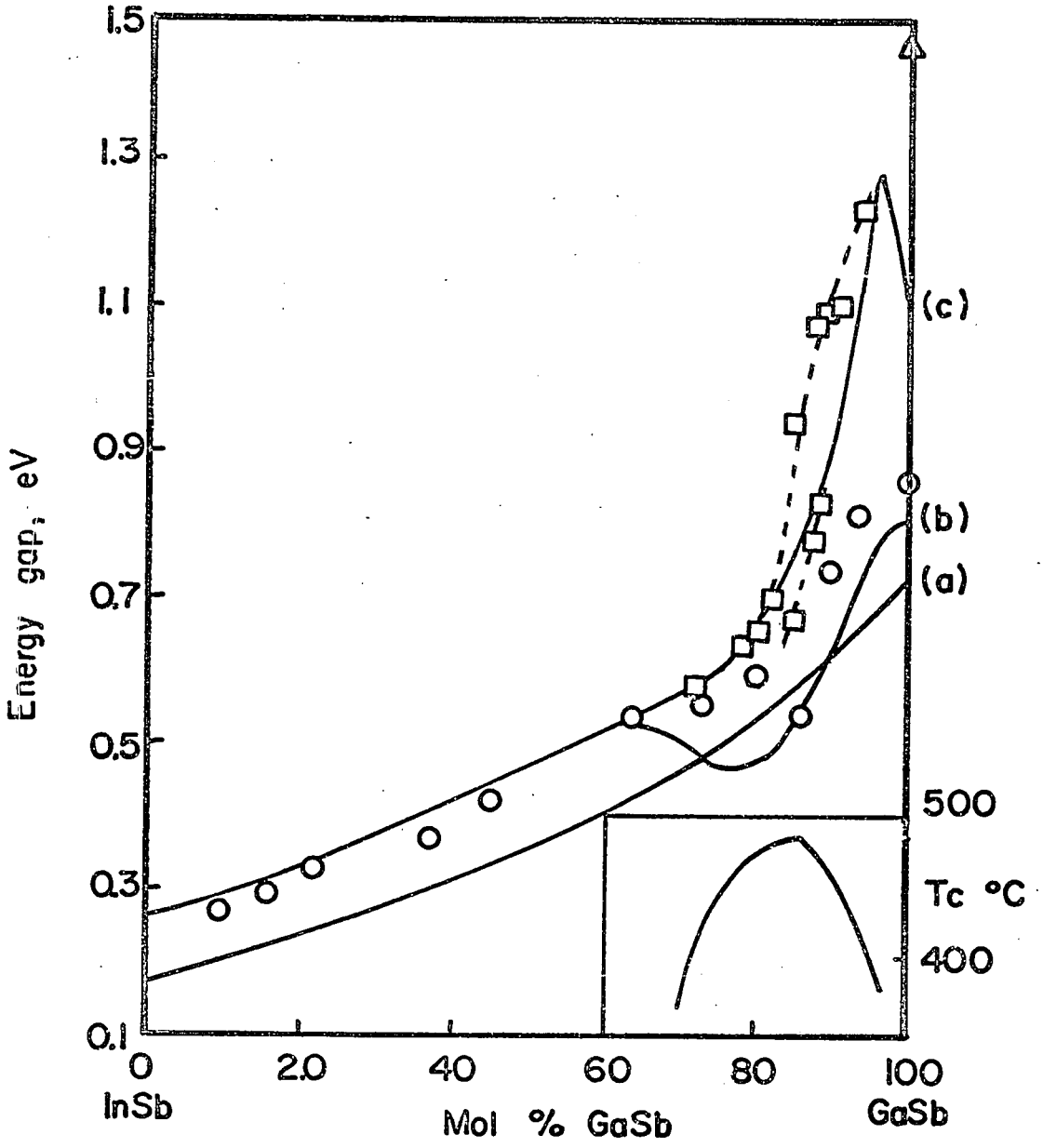

Fig. 5 Graph showing the variation with composition of:
(a) Room temperature optical energy gap,
(b)-(c) Extrapolated absolute zero of temperature electrical energy gap E_0,
O - Absolute zero of temperature optical energy gap,
Tc - Transition temperature,
△ - Blazey's result for GaSb,
□ - Present electrical results.

To ensure that the anomalous electrical results were not due to a structural effect such as a phase change, Woolley and Gillett (9) took X-ray powder photographs of GaSb at temperatures above and below the transition temperature. The photographs showed that the zinc-blende structure was retained at high temperature and the only noticeable change was the usual change in Bragg angle of the lines due to thermal expansion.

Various experimental results suggest that ordering may exist in the alloy system over the range 65-95 mol % GaSb. In such a case, the low temperature electrical energy gap would correspond to the ordered structure and the high temperature electrical energy gap to the disordered structure. The following points have been quoted, by Woolley and Gillett (9), as supporting this:

a) The form of the T_c vs. composition curve between 70 and 94 mol % GaSb is typical of the variation of ordering temperature with composition.

b) The form of the low temperature E_o curve in this composition range is similar to that observed in systems where ordering occurs (11).

c) If the graph of lattice parameter with composition for this alloy system (3) is investigated as accurately as it is possible with the present alloys, it is found to show small deviations from the Vegard line, but to intersect that line at an approximate composition of 75 mol % GaSb. It has been shown (12) that such an intersection can indicate the possibility of ordering in the vicinity of that composition.

d) The form of the solidus of the alloy system (13) indicates that the solid solution is not ideal in the composition range considered.

X-ray methods failed to show any definite origins of ordering (9), although this could be partly due to the relatively low intensity of the superlattice lines. Since the thermal conductivity of an ordered crystal is larger than that of a disordered one, an alternative method of observing the presence of ordering in these alloys was to measure their thermal conductivity and this has been carried out by Woolley and Briggs (14). Although the experimental curve of the thermal conductivity against composition did not agree very well with the theoretical curve of Abeles (15), the form of the experimental curve was not that associated with the occurence of ordering. Thus, it appears probable that long range ordering does not occur in these alloys.

1.3. Directional freezing techniques.

Physical measurements such as Hall effect and conductivity require homogeneous single phase alloys in the solid form. Because of the very slow diffusion rates in the InSb-CaSb alloys a special technique is required for their production (2). The directional freezing technique is the most useful one in this case. In this method, an ingot is placed in an asymmetrically wound furnace, so that a temperature gradient is maintained along the length of the ingot. By a controlled reduction of the temperature of the furnace a freezing surface is then swept along the ingot. The variation in composition along the directionally frozen ingot depends upon the initial gross composition of the ingot and upon the phase diagram of the InSb-CaSb alloy system. The first material to freeze out is rich in CaSb leaving the melt correspondingly richer in InSb. As the temperature is

reduced the freezing surface moves along the ingot producing alloys of progressively smaller concentration of GaSb to almost pure InSb. In order to produce homogeneous single phase alloys by the directional freezing technique it is necessary to have the freezing surface moving steadily at a suitable rate along the ingot and also a good control over the temperature of the furnace. Alloy inhomogeneity will result if the rate of movement of the freezing surface due to the lowering down of the temperature and to fluctuations in temperature control is greater than the maximum rate which would still allow equilibrium conditions to be obtained.

1.4. Properties of III-V cross-substitutional alloys.

It has been shown (16) that new semiconducting compounds can be derived from known ones by a process of cross-substitution, namely replacing one element by pairs from other groups of the periodic table while keeping the valence-electron:atom ratio constant. Thus the III-V compounds such as GaAs, InSb, etc., are derived, by this process, from the group IV elements, and the ternary compounds $ZnSnAs_2$, $CdSnAs_2$, etc., from InAs (17). In practice, several derived ternary compounds are unstable and so are not formed (18). However it is possible in these cases to carry out the process to a limited extent, for instance, in the case of InSb to replace only some of the In atoms by combinations of, say, Cd and Sn and the resulting materials can be considered as alloys between InSb and the derived ternary compound $CdSnSb_2$. It can be shown (19), from thermodynamic considerations, that InSb-$CdSnSb_2$ alloys are non-stoichiometric; some solution of Sn in the Sb lattice occurs and leaves excess Cd on the In lattice. Both the Sn and the resulting excess Cd may be expected to act as acceptors giving p-type material of high carrier concentration. Similarly InSb-In_2SnTe

alloys would be expected to give n-type material of high carrier concentration.

The cross-substitutional alloys of InSb produced by replacing In by combinations of (Cd, Sn) or (Zn, Sn) and by replacing Sb by combinations of (Sn, Te), (Sn, Se) or (Ge, Te) have been studied by Woolley and Williams (20). Limits of solid solution have been determined by X-ray and photomicrograph techniques. The Hall coefficient and optical energy gap, at room temperature, have been measured for alloys within the limit of solid solution. It was observed that as the ternary compound was added in small quantities, in the case of n-type alloy systems, the degenerate number of carriers n increased sharply to a maximum value of 9×10^{18} carriers cm^{-3}, and either remained constant at that value or decreased slowly for larger concentrations of ternary compound. A similar behaviour was observed in the variation of the optical energy gap with composition. The optical energy gap has reached a maximum value of 0.47 ev. Parrot has shown (21), from thermodynamic considerations, that the maximum value of n represents the limit of solubility of Te (or Se) in InSb. However Woolley and Williams have suggested that the maximum value of n is determined by the band structure of InSb. Many more Te (or Se) atoms than those giving this maximum value act as donors in the alloys, but the extra electrons enter much broader conduction band minima, i.e. the $\langle 111 \rangle$ minima, and are not observed by Hall effect measurements because of a much larger effective mass than electrons in the (000) minimum. The sharp increase of the optical energy gap at low ternary compound concentrations is due to the Burstein effect and because of a much higher density of states in the $\langle 111 \rangle$ minima a noticeable further increase in the optical energy gap does not occur. In the case of p-type alloys, the structure of the valence band of InSb

is such that no similar effect can occur. The highly degenerate hole concentrations produced by nonstoichiometry were observed to differ from one alloy system to another and this is determined by thermodynamic considerations similar to those given by Parrott (21).

Woolley and Williams (20) have concluded from these results that in InSb at room temperature, the <111> minima of the conduction band are 0.47 ev above the valence band maximum, and that the (000) minimum of the conduction band will accept about 9×10^{18} electrons cm^{-3} before it is so filled that electrons mainly go into the <111> minima. The similarity of the results for In_2Te_3 and In_2Se_3 alloys with InSb supports these views (22).

1.3. Theoretical background.

It is intended to outline in this section the theory used to analyse the electrical and optical results of the work described in the following chapters of this thesis. Measurements of Hall coefficient R and conductivity σ and their temperature dependence are important since R yields values of the charge carrier concentration and distinguishes between conduction by holes and electrons, and the product of R and σ yields values of carrier mobility. Also, from an analysis of the variation of R with temperature a value of the thermal energy gap can be obtained.

When a magnetic field is applied to a semiconductor carrying a current, in a direction at right angles to the current, an e.m.f. is produced across the semiconductor in a direction perpendicular to the current and to the magnetic field. This e.m.f. is called the Hall voltage and the Hall coefficient R(cm^3/coul) is given by (10)

$$R = \frac{t\,V_H}{BI} \times 10^7$$

where t(mm) is the thickness of a rectangular strip whose thickness and width are small compared with its length, V_H(mV) the Hall voltage, B(gauss) the magnetic induction field and I(ma) the current. The carrier concentration N(cm^{-3}) is given by

$$N = \frac{1}{eR} = \frac{6.28 \times 10^{18}}{R}$$

where e(coul) is the electronic charge. This equation hold exactly when the relaxation time is not a function of the velocity. Generally a numerical factor r which varies between about 1 and 2 according to the type of scattering which predominates, and also with the degree of degeneracy in a band, must be included in the above equation. The electrical conductivity σ(ohm-cm)$^{-1}$ of the semiconductor is given by

$$\sigma = \frac{Il}{VA}$$

where l(cm) and A(cm^2) are respectively the length and cross-sectional area of the strip, i(amp) the current and V(volts) the potential along l. The Hall mobility μ (cm^2/volt. sec) is defined by means of the equation

$$\mu = \sigma R$$

Since the band structure of InSb and GaSb are similar in so far as they have the extrema of the valence and conduction bands at the same place in the Brillouin zone, namely at k = 0, a simple semiconductor model will be used to calculate the thermal energy gap. From Fermi-Dirac statistics and electrical conduction theory, the total number of electrons per unit volume in the conduction band of a simple non-degenerate semiconductor is given by the equation (10)

$$n = 2\left(\frac{2\pi m_e kT}{h^2}\right)^{3/2} e^{-E_g/kT}$$

where m_e is the effective electron mass, k the Boltzmann's constant, h the Planck's constant, T the absolute temperature and E_F the Fermi level. Similarly, the hole concentration in the valence band is given by the equation

$$p = 2\left(\frac{2\pi m_h kT}{h^2}\right)^{3/2} e^{-(E_F + E_g)/kT}$$

where m_h is the effective hole mass and E_g the forbidden energy gap. If the semiconductor is intrinsic then all the electrons in the conduction band originated from the valence band and therefore n = p. The product np is then given by the equation

$$n^2 = A(m_e m_h)^{3/2} T^3 e^{-E_g/kT}$$

All the InSb-GaSb alloy specimens investigated in this thesis were n-type and according to the data of Woolley and Gillett (9), had a mobility ratio of electrons to holes much greater than unity. Hence it is reasonable to use a one carrier model in the analysis of the Hall effect results. Let us assume at first that the extrinsic carrier concentration is negligible and that measurements of the Hall coefficient R lead to the number of intrinsic carriers. Therefore

$$R = 1/ne = B(m_e m_h)^{-3/4} T^{-3/2} e^{E_g/2kT}$$

and assuming that $E_g = E_o + \beta T$ in the temperature range considered and that m_e and m_h are independent of T, the above equation can be written as

$$\ln RT^{3/2} = \ln B - 3/4 \ln (m_e m_h) + \frac{E_o}{2kT} + \frac{\beta}{2k}$$

Hence a graph of $\ln RT^{3/2}$ against $1/T$ will be a straight line in the

intrinsic region and the slope of the line gives the extrapolated thermal energy gap value E_o.

A correction must be applied to the above equation to allow for the effect of an extrinsic electron density n_e in the conduction band. This correction can be made in the following way. At any temperature T the number of carriers in the conduction band is given by $n = n_e + n_i^1$, where n_i^1 is the number of intrinsic carriers excited into the conduction band already containing n_e extrinsic carriers. Assuming that there is no acceptor impurity present, the number of holes in the valence band is equal to n_i^1. Therefore

$$np = n_i^2 = (n_e + n_i^1)n_i^1 = n(n - n_e)$$

and hence

$$R_i^2 = \frac{R^2 R_e}{R_e - R}$$

where R_e is the Hall coefficient at liquid nitrogen temperature, R the Hall coefficient at the temperature T and R_i the true intrinsic Hall coefficient. Multiplying the above equation by $T^{3/2}$ and taking the logarithm yields

$$\ln R_i T^{3/2} = \ln RT^{3/2} + \tfrac{1}{2}\ln R_e/R_e - R.$$

Thus, the latter curves of $\ln RT^{3/2}$ against $1/T$ may be corrected by adding $\frac{1}{2}\ln R_e/R_e - R$ to the ordinate at any temperature. In the above analysis it was assumed that there was no extrinsic holes in the valence band. Because of the effect of the mobility ratio these would not be observed in conduction processes but they would affect the equilibrium concentration of electrons and holes given by the product np.

If it is assumed that only one type of impurity is present in a semiconductor and the above correction is applied to allow for the presence of impurity carriers, then the energy gap obtained from a plot of $\ln np/T^3$ vs $1/T$ would be slightly higher than the value that would be obtained by allowing for two types of impurities. But the energy gap obtained by neglecting impurity carriers altogether would be slightly lower than either of these. Thus by correcting for n-type impurities (which one can measure) and by making no correction whatever, one can obtain a range of energy gap values which would embrace the correct one. It should be noted here that, when the extrinsic carrier concentration is negligible namely, in the intrinsic case, the graph of $\ln RT^{3/2}$ vs $1/T$ gives E_o even when the mobility ratio b is not large compared with unity because $R_i = (b^2-1)/ne(b+1)^2$ and the $(b^2-1)/(b+1)^2$ term is a constant which does not affect the slope of the $\ln RT^{3/2}$ vs $1/T$ graph. However when we are trying to allow for the effect of extrinsic carriers, the analysis is valid only if $b \gg 1$ because of the correction term. This acts as a limit to the accuracy of the correction term. The work of Woolley and Gillett (9) justifies the assumption that $b \gg 1$ since their results show that $b > 20$ up to 90 mol % GaSb and b falls to approximately 10 at 95 mol % GaSb.

The fundamental optical energy gap of a semiconductor is the energy required to excite an electron from the top of the valence band to the bottom of the conduction band. If the frequency ν of the incident radiation on a semiconductor is such that $h\nu \geq E_g$, the major part of the absorption will be due to electronic transitions from the valence band to the conduction band. When the frequency of the incident radiation is insufficiently high to cause band-to-band transitions i.e. $h\nu < E_g$, absorption is generally due to excitation of lattice

vibrations and to transitions between states in a single band. The latter process is usually called free-carrier absorption.

The optical energy gap can be determined from optical transmission measurements. Woolley et al (22) have devised a useful method to obtain the optical energy gap, from the variation of the transmitted radiation intensity as a function of the wavelength, for specimens of different thickness. It was assumed that the incident radiation intensity I_o is related to the transmitted radiation intensity I by the equation

$$I = I_o C e^{-kt}$$

where k is the absorption coefficient, t the thickness of the specimen and C a constant assumed independent of the wavelength in the range concerned. This gives

$$\log\left[\frac{I_o}{I}\right]_E - \log\left[\frac{I_o}{I}\right]_B = \frac{k_E - k_B}{2.303}\, t$$

where the subscript E indicates values at the wavelength λ_E, corresponding to the energy gap E_g, and the subscript B the background values. An arbitrary choice of definition of λ_E was made by putting $k_E - k_B = 300\ cm^{-1}$. This choice gave values of E_g for InAs and other semiconducting compounds close to the accepted values. Therefore, the optical energy gap can be determined by means of the above equation and a graph of $\log(I_o/I)$ against wavelength.

1.6. Aims of the present work.

Up to now the electrical and optical properties of the InSb-GaSb alloy system have been investigated using p-type alloys only. It was intended to prepare some polycrystalline n-type InSb-GaSb semiconducting alloys and to measure the Hall coefficient and electrical

conductivity in order to try to explain the anomalous results described in section 1.2 of this chapter. The preparation of the InSb-GaSb alloys requires a long period of time. During that time the In_2SnTe_3-InAs alloy system was investigated in order to determine the height of the second lowest conduction band minima above the valence band of InAs. This system has been investigated because it was a part of a programme of research, on the cross-substitutional alloys, carried out by E. W. Williams under the direction of Dr. Woolley. All the work described in this thesis is part of a programme of research into the properties of alloy semiconductors carried out at the Department of Physics of the University of Ottawa under the direction of Dr. J. C. Woolley.

Chapter 2

Preparation of n-type InSb-GaSb Semiconducting Alloys

2.1. Preparation of the III-V semiconducting compounds InSb and GaSb.

The InSb used to prepare the alloys was obtained from the Consolidated Mining and Smelting Company of Canada Limited. It was supplied in the form of polycrystalline ingots, doped with Te, and was n-type with 2.4×10^{16} carriers cm^{-3} and a resistivity of 0.004 ohm-cm at room temperature.

The GaSb was made in 30 gram ingots from 99.999% purity Ga and Sb. The stoichiometric amounts of the elements were weighed out, evacuated in a quartz tube down to a pressure less than 10^{-5} mm. of mercury and sealed off by means of an oxy-acetylene torch. The quartz tube was suspended by means of a Kanthal wire in a melting furnace, for 30 minutes, at a temperature of approximately 1000°C which is above the melting point of the constituent elements and of the compound itself. The tube was occasionally shaken during the melting to ensure complete mixing. Finally, the mixture was quenched in air. The GaSb prepared in this way was found, from Hall coefficient measurement, i.e. assuming that $n = 1/eR$, to be p-type with 5×10^{17} carriers cm^{-3} at the centre of the ingot. Unless purposely doped, GaSb is always p-type. This p-type behaviour is probably due to an excess of Ga which is incorporated into the lattice giving rise to p-type carriers although, it may equally be due to acceptor impurity with a segregation coefficient equal to 1 (23).

A vacuum system was built for sealing off quartz tubes. It consists essentially of a 2" oil diffusion pump, a backing pump, a vacuum gauge and inlets where the tubes to be evacuated and sealed off are connected.

2.2. Description of the directional freezing furnace and control of the furnace temperature.

The heating element of the directional freezing furnace was made of number 17 B and S Kanthal wire suitably wound on a "Mullite" refractory tube of 2" in diameter and 22" long. The correct winding for a linear temperature gradient of 6°C per cm. extending over some 25 cm. was found by trial and error. The winding was covered with a $\frac{1}{2}$" layer of high temperature refractory cement. The tube was mounted in a fire-proof box, the end of the box were made of 1 square foot asbestos boards and the sides of a 1/32" thick aluminum sheet. The casing was filled with "Vermiculite" as a heat insulator. A Pt/Pt13%Rd thermocouple was used to control the furnace temperature. The hot junction of the thermocouple was cemented between two turns of the winding at the hot end of the furnace and the cold junction was placed in running water. The temperature profile along the directional freezing furnace is shown in Fig. 6, also shown is the number of turns of wire per inch and the position of the ingot in the furnace.

Two directional freezing furnaces have been built. The temperature of one of them was controlled by a two positions or on/off Kelvin and Hughes temperature controller accurate to $\pm$ 1°C. The control of the temperature of the other furnace was achieved by a continuous current Ether temperature controller accurate to $\pm$ .1°C. It is a controller which proportions the electrical power into the furnace to maintain control thereby reducing overshoot and undershoot encountered with the on/off controller. Finally, the temperature of the furnaces was lowered at a rate of 4°C per day by means of a "meccano" part gear system connected to the control knob of the temperature controller.

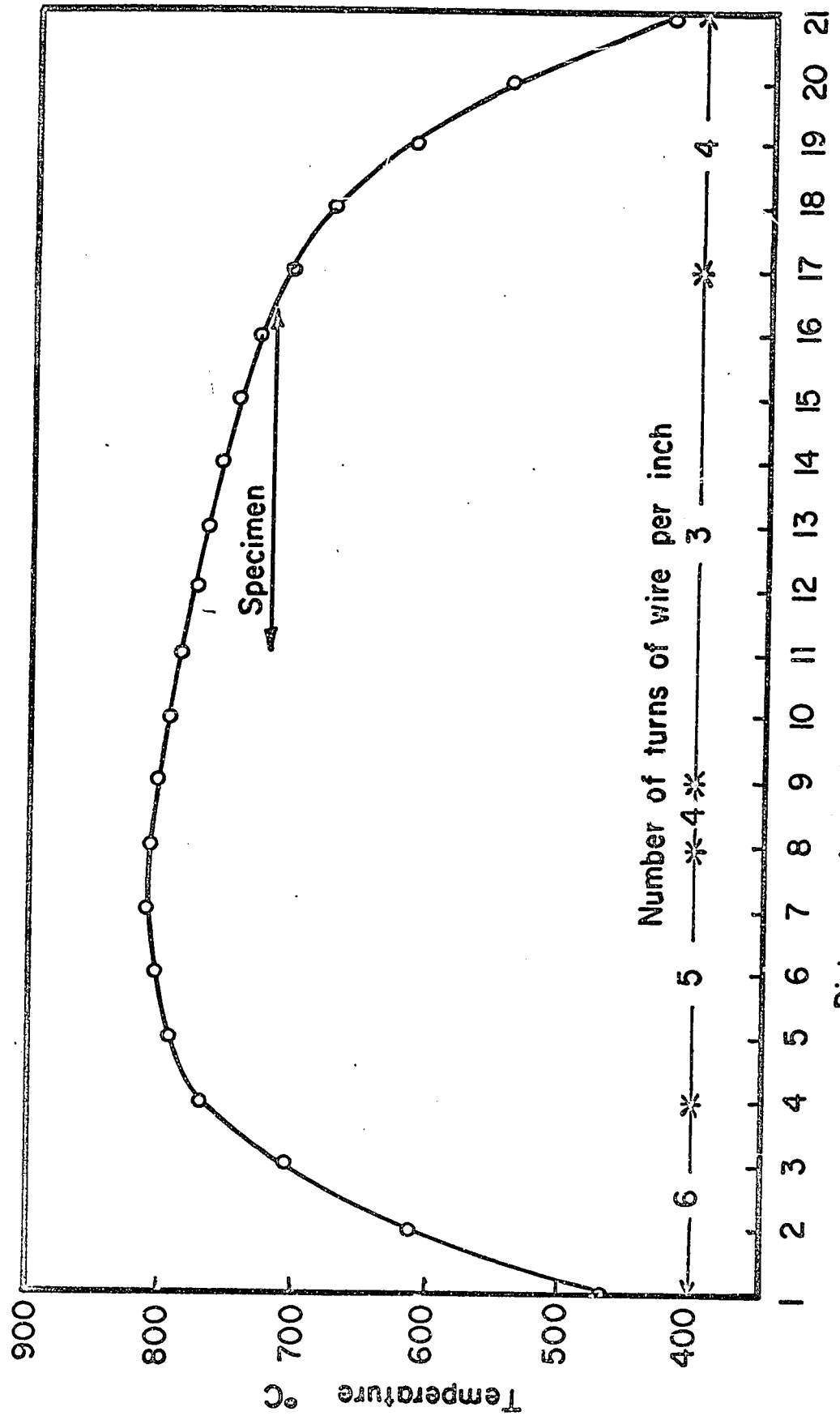

Fig. 6 Temperature profile along the directional freezing furnaces.

2.3. Preparation of directionally frozen ingots.

A 40 gram amount of 50 mol % InSb-50 mol % GaSb doped with 0.6 milligram of Te was sealed in an evacuated quartz tube, melted at about 900°C and allowed to cool to form a solid ingot along the length of the 13 cm. long quartz tube. The tube and its content were then placed in an asymmetrically wound furnace described in the previous section. The exact position of the ingot in the furnace is shown in Fig. 6. The cold end of the furnace was set slightly above the melting point of GaSb. The gear system was then switched on and the furnace temperature slowly reduced at a rate of 4°C per day until the high temperature end of the ingot was at 500°C which is below the melting point of InSb, the whole process taking two months. The ingot was then removed from the furnace for analysis. An ingot of 30 mol % InSb-70 mol % GaSb doped with about 1.5 milligram of Te was also prepared in the same way.

The ingot was taken out of the quartz tube and stuck, with "glyptal cement", on a rectangular "arborite" slab. In order to obtain specimens for electrical measurements and also material to X-ray, slices of approximately 1 mm thickness were cut from several places along the ingot with a carborundum wheel cutter. This cutter was made in the workshop of the physics department. It consists of a 3" diameter carborundum wheel 0.010" thick driven by an electric motor at 4500 r.p.m., a turn-table moving in three directions and a pump bringing a mixture of soluble oil and water to the cutting wheel. The mixture was used as a lubricant. The slices were then stuck on smaller "arborite" blocks and two specimens in the form of rectangular strip of dimensions 7x1x1 mm. were cut with the

carborundum wheel cutter. The material was taken off the blocks by dissolving the glue with acetone. The specimens were observed to be free from defects and had a good mechanical strength although they were somewhat brittle. Small pieces from each slices were powdered and X-rayed with a 11.483 cm Debije Scherrer ~~powder~~ camera using CuKα radiation in order to obtain the composition and homogeneity of each specimen. The lattice parameter was determined from the X-ray photographs with a vernier travelling microscope and the composition, from a graph showing the variation of the lattice parameter against the composition. Such a graph is shown in Fig. 1. The variation of composition with distance along both directionally frozen ingots is shown in Fig. 7. Most X-ray pictures showed sharp lines with the Cu $K\alpha_1$, $K\alpha_2$ doublet resolved in high Bragg angle lines. This was an indication of homogeneous alloys. However, the X-ray pictures of the alloys from inget A in the composition range 75-80 mol % GaSb showed traces of a second phase, and the alloys from ingot B in the composition range 50-60 mol % GaSb gave blurred lines indicating that they had some degree of inhomogeneity. In inget A, single phase specimens in the composition range 75-80 mol % GaSb would probably have been obtained by using a better control over the temperature and a slower movement of the freezing surface. In ingot B, the blurring of the lines in the composition range 50-80 mol % GaSb is due to the rapid decrease in composition along the ingot in that region. Homogeneous alloys in this composition range can be obtained by using a different initial composition. For electrical measurements, in the composition range 70 - 87 mol % GaSb and 87 - 94 mol % GaSb specimens were taken from ingot A and B respectively. The reasons for this selection will be stated in the next chapter.

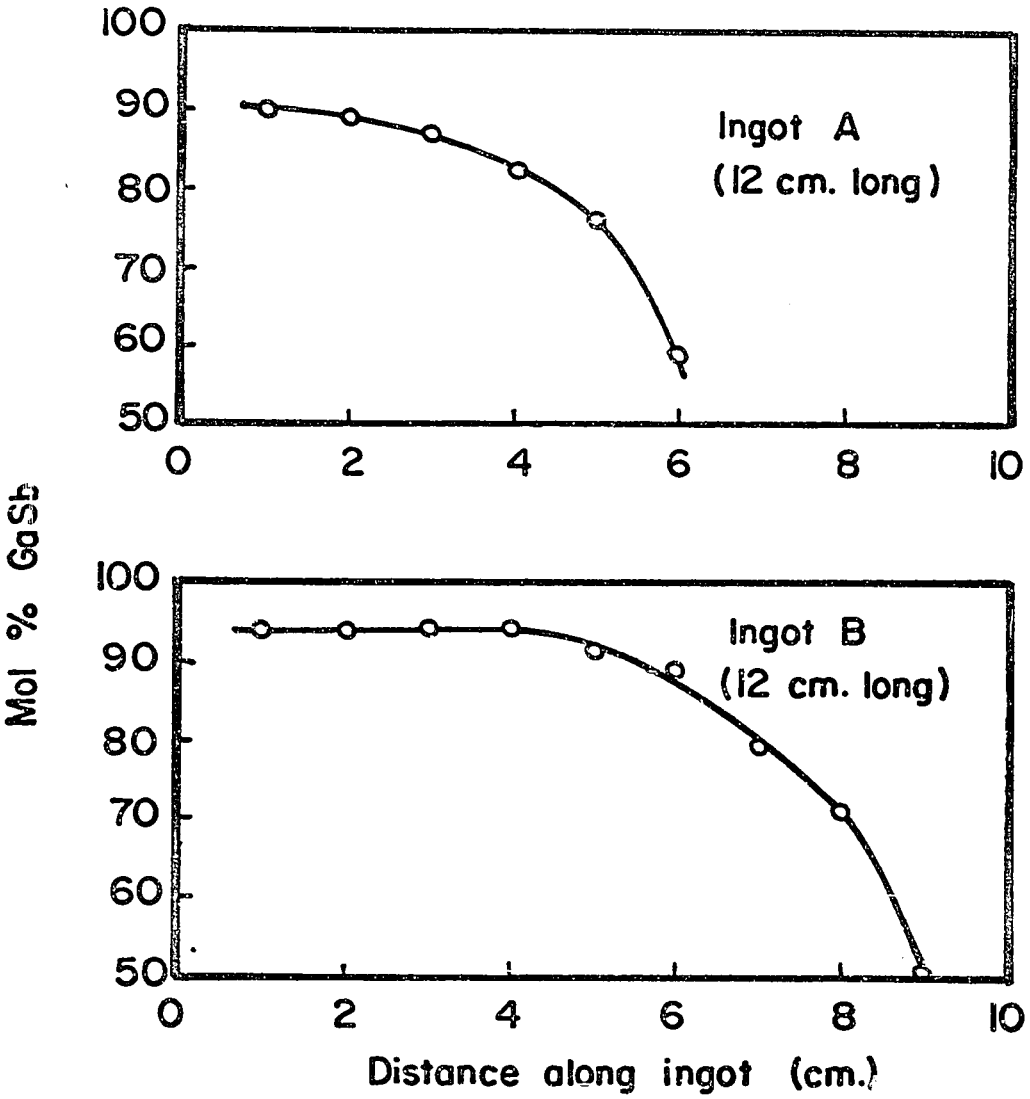

Fig. 7 Variation of composition as a function of position along a directionally frozen ingot. Ingot A, mean composition 50 mol % GaSb 50 mol % InSb, ingot B, mean composition 70 mol % GaSb 30 mol % InSb.

Chapter 3

Electrical Measurements on n-type InSb-GaSb Semiconducting Alloys

3.1. Introduction

Measurements of Hall coefficient and conductivity as a function of temperature were made on alloys in the composition range 72-96 mol % GaSb because, it was seen in section 1.4 of chapter 1 that, an anomalous behaviour occurs in that composition range.

3.2. Description of the apparatus

In order to measure the Hall coefficient and conductivity at high temperature a suitable high temperature vacuum furnace and specimen holder were built. A diagram to scale of the specimen holder built by the workshop of the physics department is shown in Fig. 8. It was made of non-magnetic stainless steel and the specimen was resting on a small slab of pyrophilite fixed to one end of the holder. The current was passed through the specimen by two steel pressure contacts, one contact was fixed and the other spring loaded by a coil compression spring which was situated at the other end of the holder. The Hall and potential probes of platinum wire were spark welded to the specimen at the appropriate positions. The temperature was measured by a Pt/Pt 13% Rd thermocouple situated very close to the specimen. The thermocouple leads, and the copper leads connected to the pressure contacts and to the Hall and potential probes were brought out of the holder through insulating alumina rods.

The specimen holder fitted into a high temperature furnace which was placed between the flat pole pieces of an electromagnet.

Fig. 8 Hall specimen holder

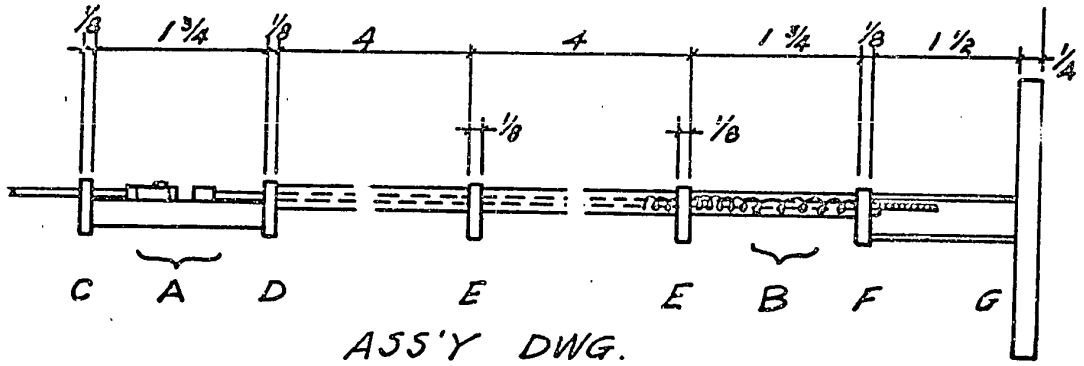

ASS'Y DWG.

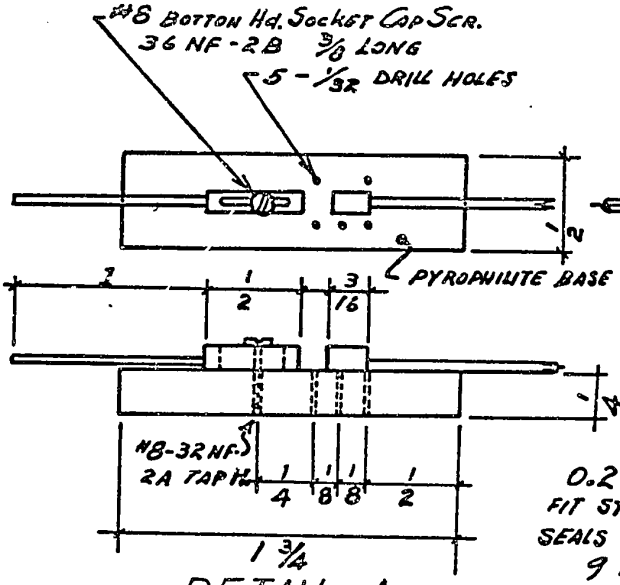

DETAIL A

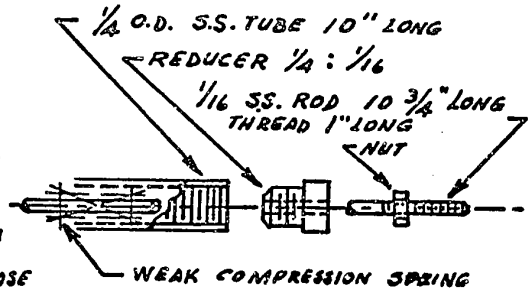

DETAIL B

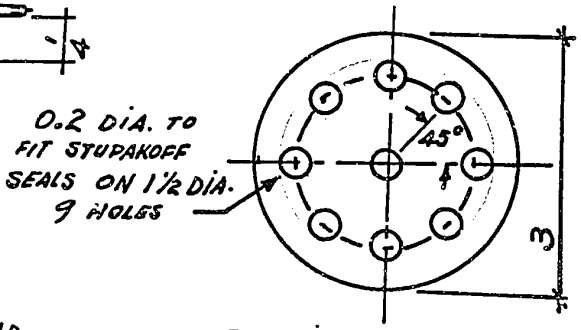

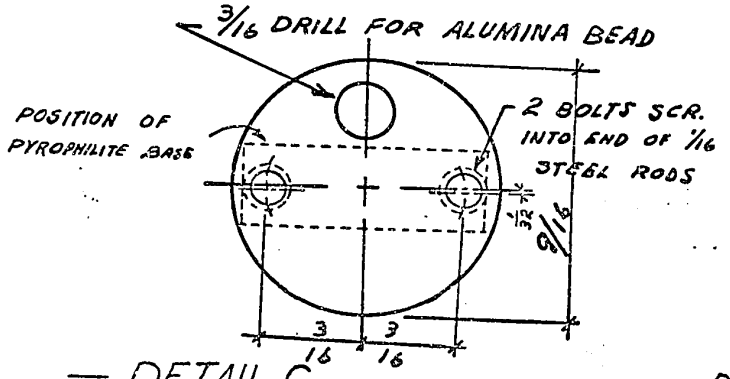

DETAIL C

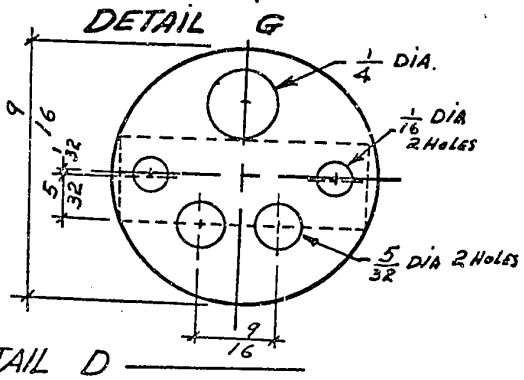

DETAIL D

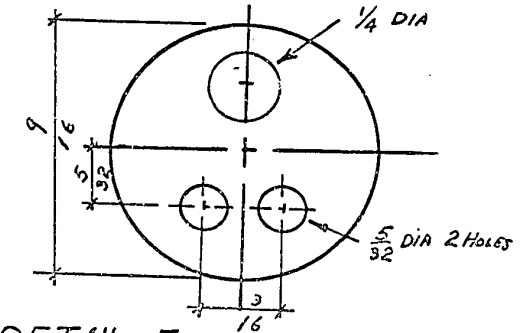

DETAIL E

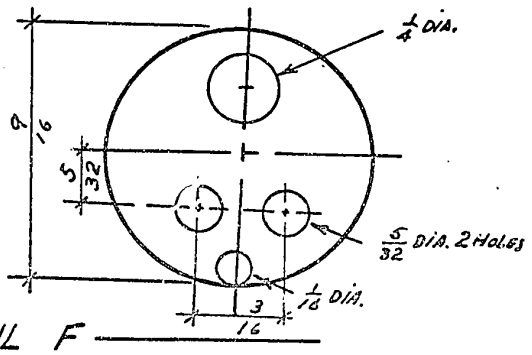

DETAIL F

The furnace was made by winding number 17 B and S Chromel A wire on a "Mullite" refractory tube, covering the winding with refractory cement and surrounding the heating element with a water jacket as shown in Fig. 9. The specimen holder fitted on to an O-ring vacuum seal at one end of the furnace and the furnace was evacuated by means of a small vacuum system which was connected at the other end as shown in Fig. 9. A pressure less than 0.5 mm of mercury was obtained and this was sufficient to prevent specimen oxidation at 700°C. The temperature of the furnace was controlled by means of an on/off Kelvin and Hughes temperature controller accurate to $\pm$ 1°C.

In order to facilitate the measurements of the various voltages involved in the determination of the Hall coefficient, conductivity and temperature, a switch board was wired as shown in Fig. 10. All voltage measurements were made with a Rubicon potentiometer which was accurate to $\pm$ 1 μV. The current through the specimen was determined by measuring the voltage across a standard 10 ohms resistor in series with the sample. Due to the non-alignment of the Hall probes, a voltage was developed across them when the magnetic field strength was zero. This apparent Hall voltage was backed off by a balancing circuit as shown in Fig. 10. When a magnetic field was applied, the voltage measured across the Hall probes was then a true Hall voltage. The electromagnet was calibrated by means of a Rawson-Lush rotating coil gaussmeter.

3.3. Experimental procedure.

For the measurements of the Hall effect and conductivity, specimens in the form of rectangular blocks of dimensions 7x1x1 mm were etched in CP4 in order to clean the surfaces. Etchant CP4 consist of: 45 parts concentrated nitric acid, 27 parts glacial acetic

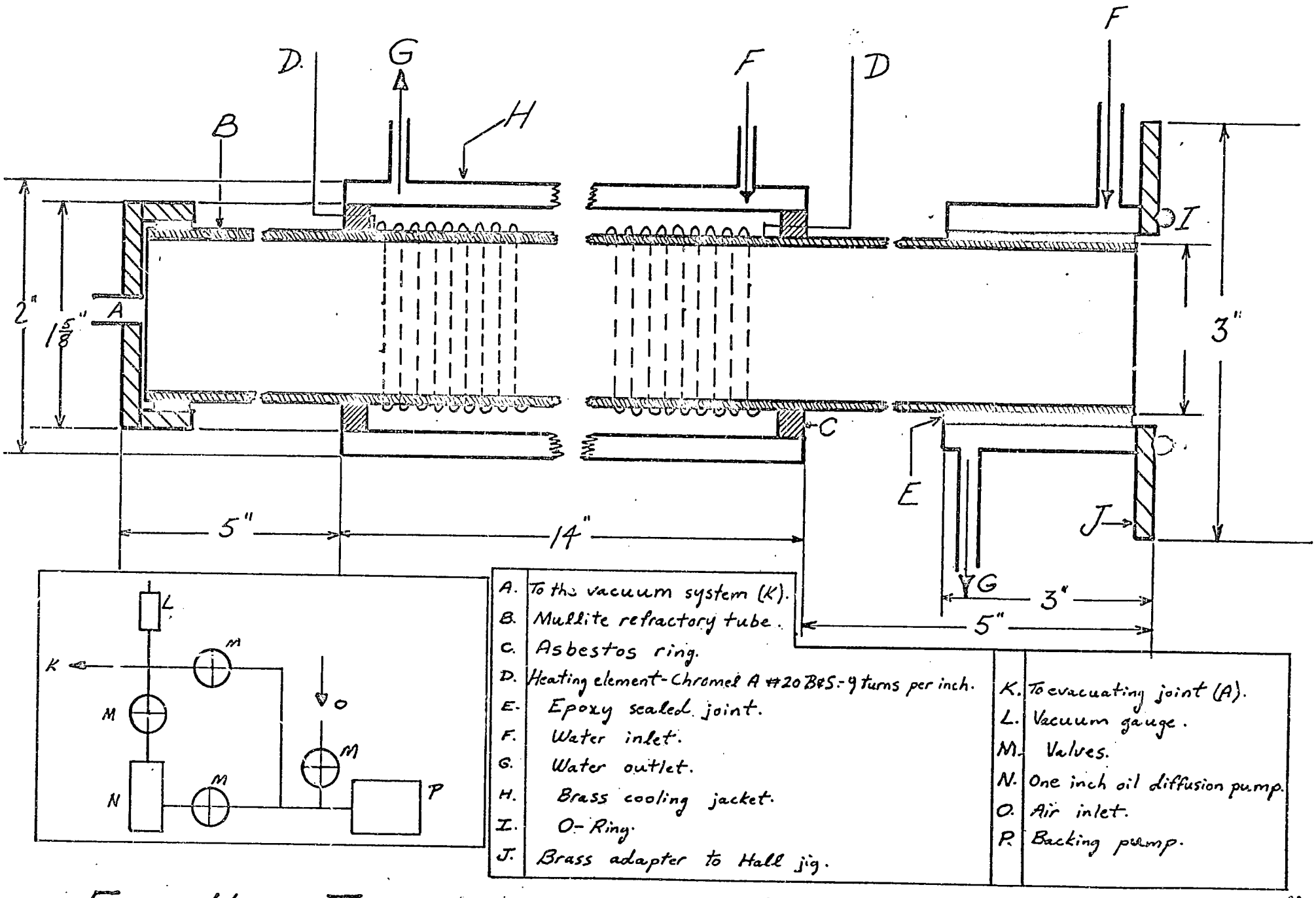

A.	To the vacuum system (K).
B.	Mullite refractory tube.
C.	Asbestos ring.
D.	Heating element - Chromel A #20 B&S - 9 turns per inch.
E.	Epoxy sealed joint.
F.	Water inlet.
G.	Water outlet.
H.	Brass cooling jacket.
I.	O-Ring.
J.	Brass adapter to Hall jig.

K.	To evacuating joint (A).
L.	Vacuum gauge.
M.	Valves.
N.	One inch oil diffusion pump.
O.	Air inlet.
P.	Backing pump.

FIG. 9 HIGH TEMPERATURE HALL FURNACE.

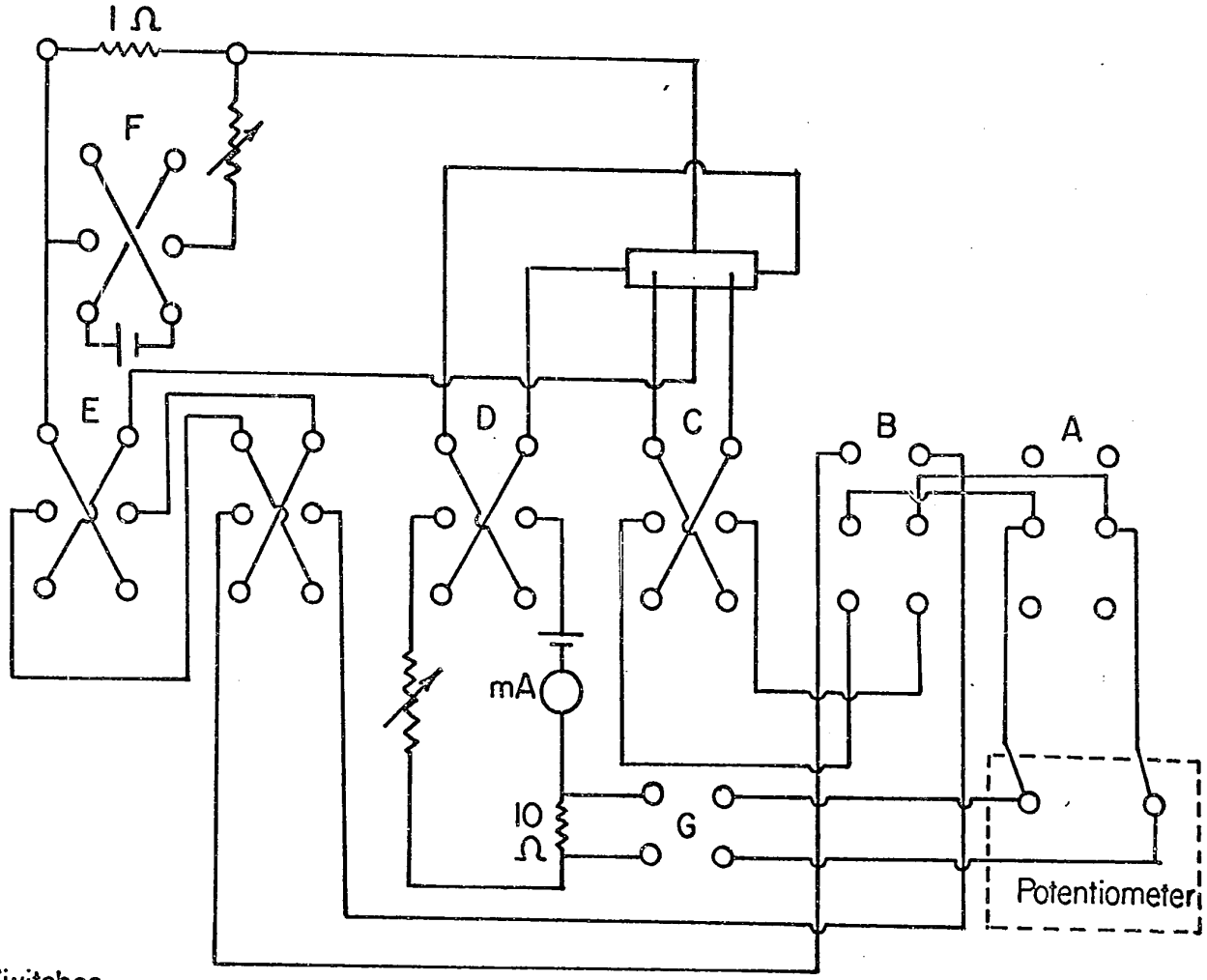

Switches :

A: Temperature measurement
B: Hall voltage „
Potential „
C: Positive potential
Negative „
D: Positive current
Negative „
E: Positive Hall voltage
Negative „ „
F: Positive back-off voltage
Negative „ „
G: Current measurement

Fig. 10 CIRCUIT DIAGRAM OF ELECTRICAL APPARATUS

acid, 27 parts 48% hydrofluoric acid and 1 part bromine. The production of the specimens has been described in section 2.3 of chapter 2. A specimen was then placed in the Hall holder between the two current pressure contacts and the platinum probes were spark welded to the specimen in the appropriate position to measure the Hall voltage and potential drop along the sample. To avoid end-effect problems, the dimensions of the sample must and were such that the length-to-width ratio was greater than 4, with the potential probes located a distance from the ends at least equal to the width of the sample. A current of approximately 60 ma. was passed through the specimen and an electromagnet was providing a suitable magnetic field. The value of the magnetic field strength used was such that the simple formula for the Hall effect remained valid. In the derivation of the equation $R = 1/ne$, second order terms, involving the product of $\mu x B$, were ignored. This may be done if $\mu B < 1$ and this condition was satisfied, for a given specimen, by choosing an appropriate value of B. In order to get the extrinsic carrier concentration, a Hall effect measurement was carried out at liquid nitrogen temperature, by lowering the specimen holder in a dewar of liquid nitrogen, placed between the pole pieces of an electromagnet. The specimen holder was afterwards allowed to dry and placed in the high temperature furnace which was evacuated to a pressure less than 0.5 mm of mercury. Hall effect and conductivity measurements were carried out at 20°C temperature intervals, in the intrinsic region, from 300°C to a temperature close to the melting point of the alloy. The temperature was kept steady within 1°C during each measurement. Four Hall voltages were measured at each temperature, one for each combination of current and magnetic field direction, the average of these four voltages is independent of all effects other than second order ones.

The distance between the potential probes of the specimen was measured with a vernier travelling microscope and its thickness and width with a micrometer. The measurements were carried out on some 10 specimens in the composition range 72-94 mol % GaSb and they were analysed as indicated in section 1.5 of chapter 1. The results will now be considered in the next section.

3.4. Results.

It must be recalled that it was seen in section 1.5 of chapter 1 that:

$$\log R_i T^{3/2} = \log R T^{3/2} + \tfrac{1}{2} \log R_e/R_e - R$$

where R_i is the true intrinsic Hall coefficient, R the measured Hall coefficient and $\frac{1}{2} \log R_e/R_e - R$ the correction factor allowing for the effect of an extrinsic electron density in the conduction band. The effect of the correction factor can be seen from the graphs of $\log R_i T^{3/2}$ and of $\log R T^{3/2}$ against $1/T$ for typical alloys; these graphs are shown in Fig. 11. It is also seen that one graph (b) is linear over the entire intrinsic region and that the other (a) breaks into two linear parts in the intrinsic region. The points which lie outside the straight lines at lower temperatures are due to the following factors: (i) as the temperature was decreasing the extrinsic behaviour started to be observed and (ii) the correction factor for the effect of an extrinsic electron density in the conduction band has the tendency to pull the points outside the straight line. The variations of the extrapolated absolute zero of temperature electrical energy gap with composition is shown in Fig.5&11a.The electrical and optical results of Woolley et al for the p-type alloys are also shown in Fig. 5. It is seen that for

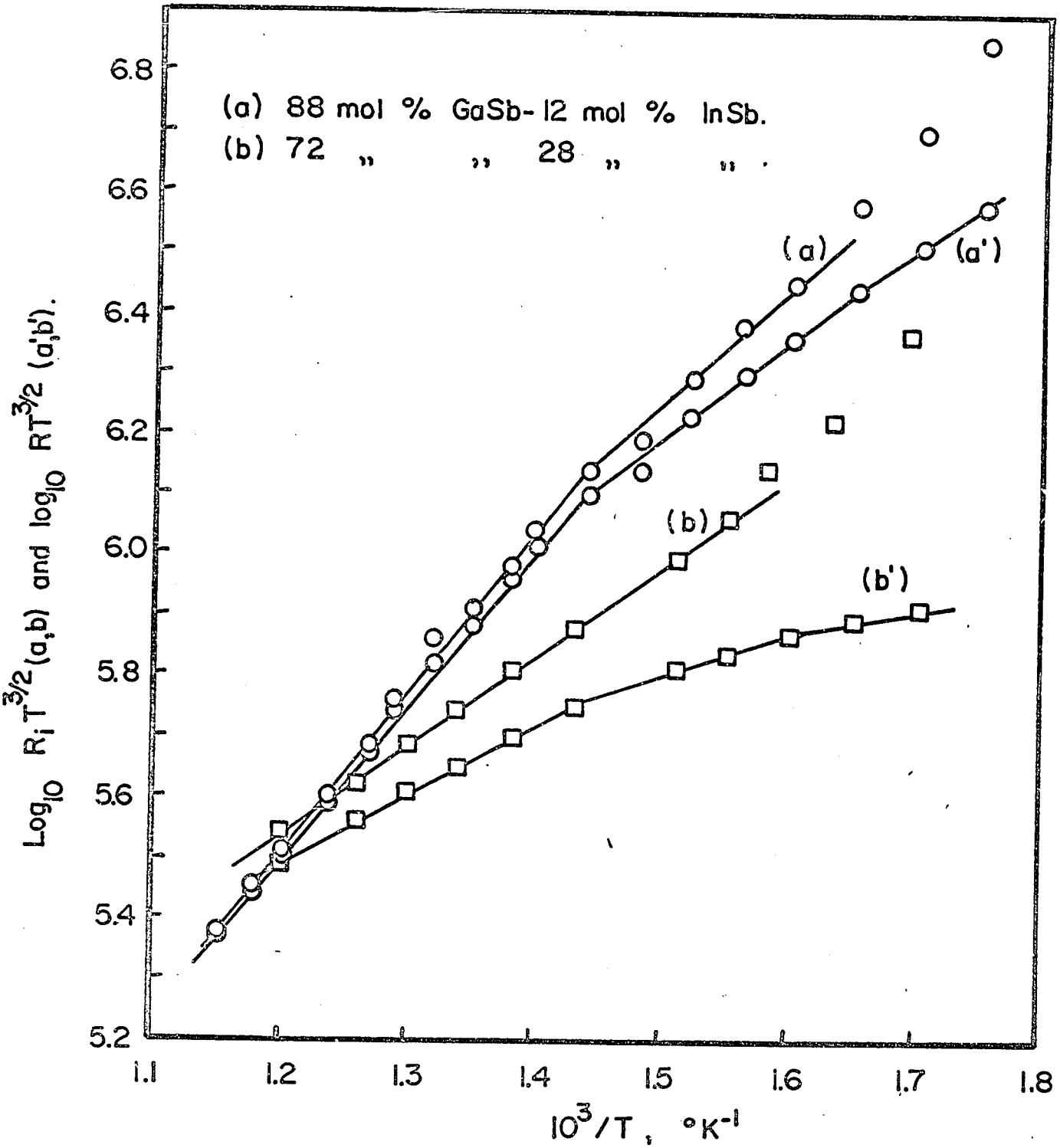

Fig. 11 Log_{10} $R_i T^{3/2}$ and log_{10} $RT^{3/2}$ vs $10^3/T$ for typical alloy specimens.

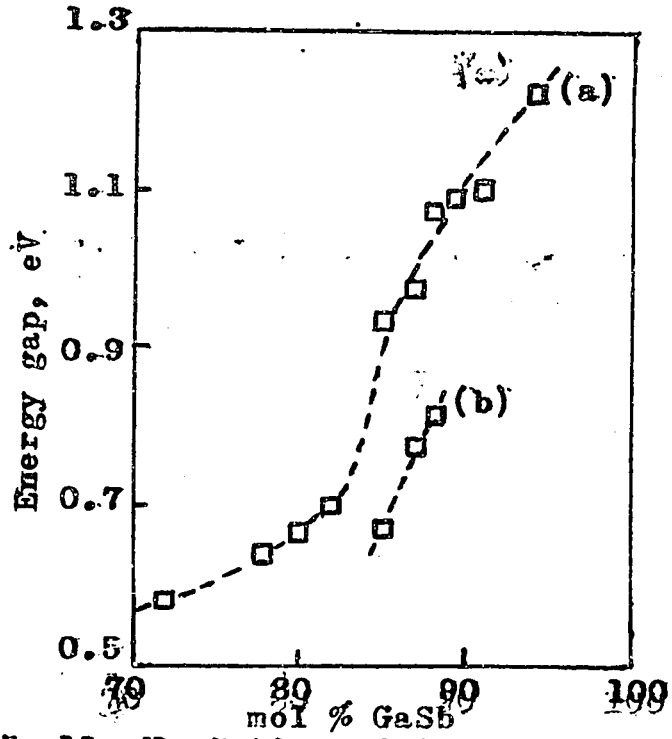

Fig.11a Variation of the extrapolated absolute zero of temperature electrical energy gap with composition for the n-type alloys.
(a) "high" temperature results,
(b) "low" temperature results.

compositions between 72 and 82 mol % GaSb the present results agree with the ones of Woolley and Gillett. A low temperature electrical energy gap was not obtained from the present measurements because the extrinsic carrier concentration was too high i.e. the intrinsic behaviour was observed near or above the transition temperature T_e. A graph of the variation of the extrinsic carrier concentration with composition and position along ingot A is shown in Fig. 12. One observed that the extrinsic carrier concentration increases as the GaSb concentration decreases. It is also seen from Fig. 3 that for compositions between 87 and 94 mol % GaSb the low and high temperature electrical energy gaps do not agree with the electrical results of Woolley and Gillett but the present low temperature electrical energy gaps seem to agree with the optical results of Woolley and Evans. One must remember that there is a certain amount of inaccuracy in the present low temperature values because of the factors discussed above and of the approximations discussed in section 1.5 of chapter 1. A low temperature electrical energy gap was not obtained for compositions between 89 and 94 mol % GaSb for the reason stated previously. The transition temperature T_e obtained from the present results is approximately 430°C which is different by 50°C from the value obtained by Woolley and Gillett for p-type alloys. It was seen in section 1.4 of chapter 1 that this transition was not due to a structural transformation then it is not surprising that the same transition temperature was not obtained and in fact it will be seen in the next section of this chapter that this transition is due to a band change. For compositions between 89 and 94 mol % GaSb the Hall effect and conductivity measurements were made on specimens taken from ingot B and specimens of lower composition were not used

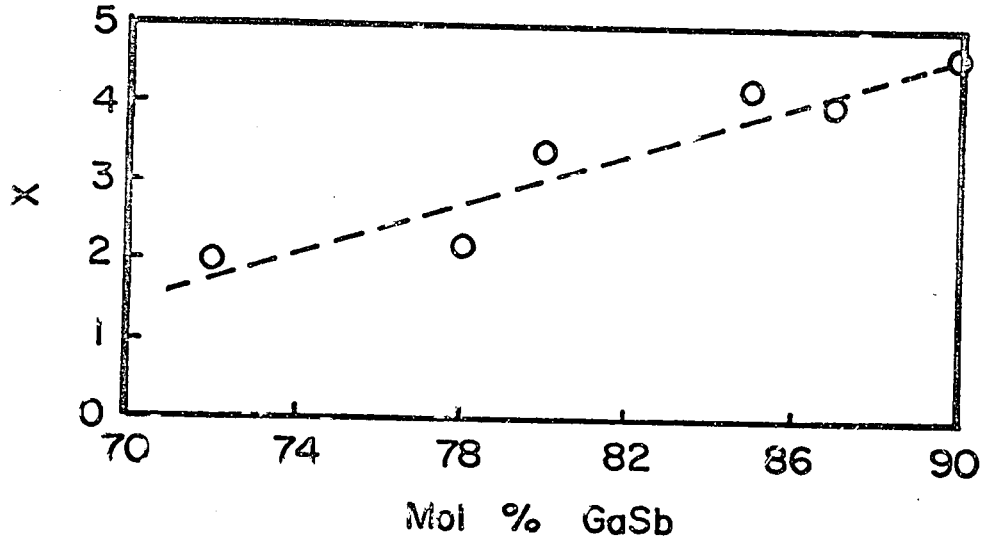

Fig. 13 Variation of mobility temperature exponent x with composition.

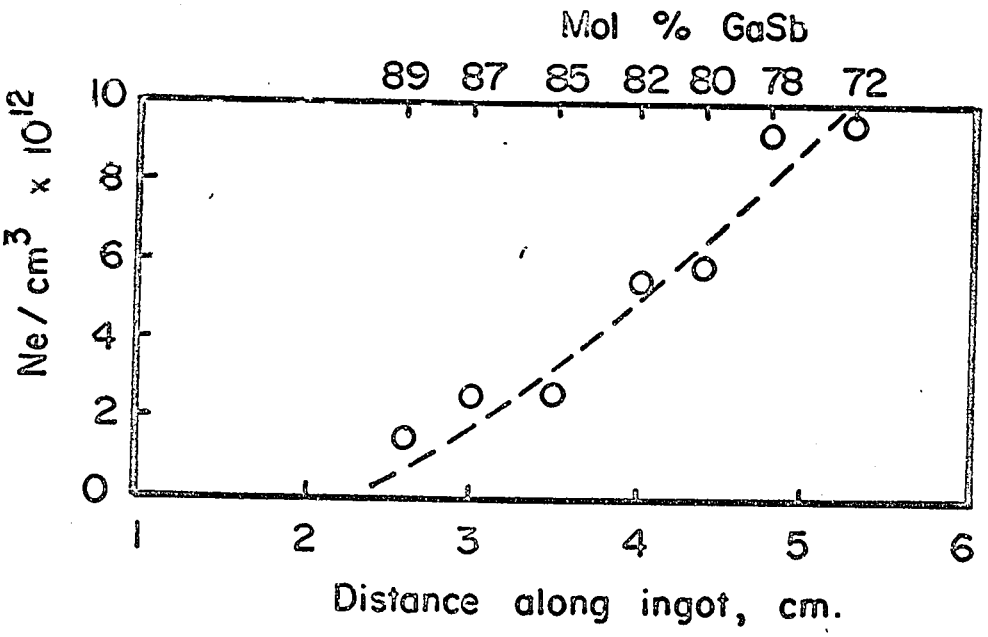

Fig. 12 Variation of extrinsic carrier concentration Ne with position along ingot A (mean composition 50 mol % GaSb – 50 mol % InSb).

because the large extrinsic carrier concentration masked the intrinsic behaviour. For the other compositions the specimens were taken from ingot A.

The Hall mobility μ_H was obtained from the product of the Hall coefficient and conductivity. Graphs of the variation of $\log \mu_H$ against $\log T$ for typical alloys are shown in Fig. 14. It is seen that these graphs are linear at high temperature and that the Hall mobility decreases as the InSb concentration decreases. Applying the relation $\mu_H = \text{constant} \times T^{-x}$ to these results a high temperature value of x was obtained for each of the alloys. A graph of the variation of the mobility temperature exponent x with composition is shown in Fig. 13, and it is seen that x decreases as the GaSb concentration decreases. The results will now be discussed in the next section.

3.5. Discussion of the results.

Before any attempt to explain the electrical properties of the alloys, the properties of GaSb itself must be explained. The electrical properties of p-type GaSb have been measured by Woolley and Gillett (9) and by Blasey (24). A low and a high temperature electrical energy gap was obtained as in the case of the 65-100 mol % GaSb alloys. A graph of $\log np/T^3$ vs. $1/T$ is shown in Fig. 15. Blasey has carried out an analysis of the electrical results using Sagar's conduction band model of GaSb (25). The intrinsic region was considered as being split into two parts. In the low temperature section, the conduction is carried out by the holes in the valence band and electrons in the conduction band minimum at $k = 000$ only. At higher temperature, the electrons excited into the conduction band minima in the $\langle 111 \rangle$ directions, as well as the other two types of carriers, contribute appreciably to the conduction processes. Blasey has

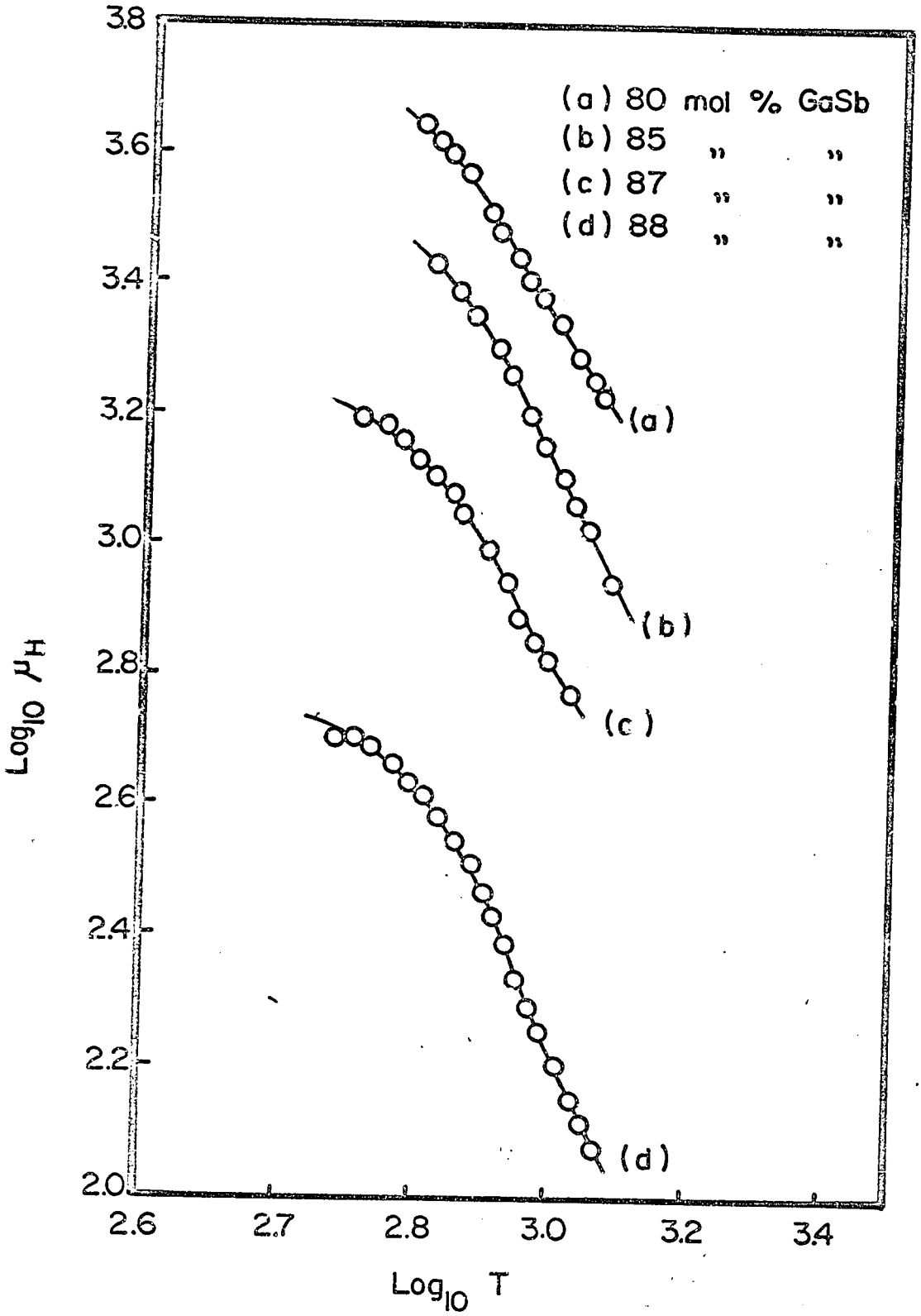

Fig. 14 $Log_{10}\ \mu_H$ vs log T for typical alloys.

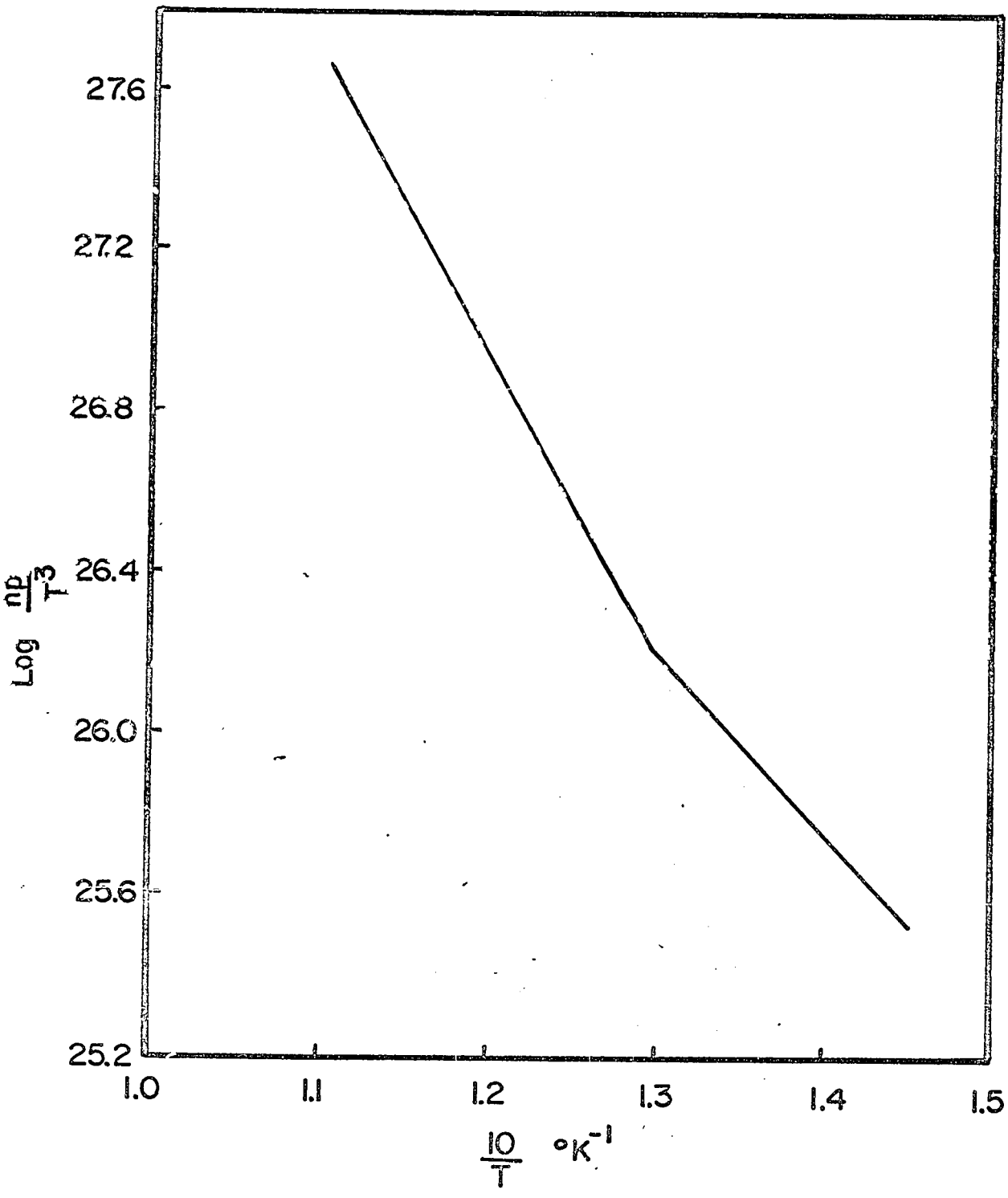

Fig. 15 Variation of log np/T^3 vs $10^3/T$ for GaSb (after Blazey)

arrived at the following equation

$$Ce^{\Delta E/kT} = \frac{(b_1-1)-2Ren_o(b_o+1)-2Rep_e}{2Ren_o(b_1+1)} + \frac{\sqrt{(b_1-1)^2+4Ren_o(b_o-b_1)(b_o+1)+4Rep_eb_1}}{2Ren_o(b_1+1)}$$

where C is a constant, ΔE the energy separation of the two conduction band minima, b_1 the mobility ratio of the electrons in the ⟨111⟩ minima and holes in the valence band, b_o the mobility ratio of the electrons and holes at k = 000, R the Hall coefficient, e the electronic charge, p_e the hole density due to impurities and n_o the intrinsic number of carriers in the conduction band minimum at k = 000. Blacey's analysis is given in the Appendix at the end of this thesis. From the measured values of the Hall coefficient the value of $Ce^{\Delta E/kT}$ was calculated as a function of temperature. The slope of the graph of $\log Ce^{\Delta E/kT}$ against $^1/T$ gave the energy separation $\Delta E = 0.52eV$ of the two conduction band minima at 0^oK. The value quoted by Sagar (25) for ΔE is 0.08eV at room temperature. Therefore the temperature coefficient is $-1.5\times10^{-3}eV/^oK$. This is in poor agreement with the value of $-3\times10^{-4}eV/^oK$ given by Sagar (25). Also more recent workers (26) have given evidence that the separation of the band minima decreases at a rate of $10^{-4}eV/^oK$ as the temperature is decreased. This latter value would predict an energy separation of about 0.05eV at 0^oK, a factor of ten smaller than the result of the above analysis. Blacey has carried out his treatment of GaSb up to that point.

In the present thesis, two corrections have been applied to Blacey's treatment of GaSb and the analysis has been applied to the conduction band minima in the ⟨100⟩ directions instead of the ⟨111⟩

direction; this has finally yielded successful results. The form of the electrical results for GaSb has been explained and this has been used with some other experimental and theoretical results in order to explain the variation of the electrical energy gap of the InSb-GaSb alloys as a function of composition.

First, let us consider the two corrections. The relation between b_o and b_l used by Blaney was that given by Sagar (26), namely $b_o = 6b_l$. At present the accepted value is $b_o = 15b_l$. In the determination of, n_o, the intrinsic number of carriers in the conduction band minimum at k = 000, Blaney has neglected, n_l, the intrinsic number of electrons in the conduction band minima in the <111> directions. This has been taken into account in the following way. The number of holes is given by

$$p = n_o + n_l + p_e$$

and the product $n_o p$ is given from the graph of $\log n_o p/T^3$ vs. $1/T$. The product $n_o p$ can be written as

$$n_o p = n_o(n_o + n_l + p_e) = A$$

where $n_l = n_o \cdot e^{\Delta E/kT} = n_o Y$. Thus n_o is given by

$$n_o = \frac{-p_o + \sqrt{p_o^2 + 4(1+Y)A}}{2(1+Y)}$$

The Hall coefficient R for the three types of carriers is given by

$$R_H = \frac{n_o(b_o^2 - 1) + n_o(b_l^2 - 1)Y - p_o}{\left[n_o(b_o + 1) + n_o(b_l + 1)Y + p_o\right]^2}$$

The meaning of the symbols in the above formulae is the same as

before. Now a value of Y for various temperatures can be obtained by graphical solution. Thus writing

$$F(Y) = Re\left[n_o(b_o+1) + n_o(b_1+1)Y + pe\right]^2 - n_o(b_o^2-1) - n_o(b_1^2-1)Y - p_e$$

one can draw a graph of $F(Y)$ against Y and find the value of Y where $F(Y)$ is zero. This has been done for various temperatures and a graph of log Y vs $^1/T$ has been plotted as shown in Fig. 16. The results of Blaney's calculations are also shown in this Figure. It is seen that although Blaney's equation was incorrect and also the ratio of b_o/b_1 used was wrong and hence the values of Y are different from the present ones, the slopes of the two curves are still practically the same, apparently by coincidence. Hence the value of ΔE from the present calculations is still 0.52eV.

Secondly, the corrected analysis will now be applied in the following way. It is known that the <111> minima are still very close (0.06eV) to the (000) minimum at absolute zero (26). The value of $\Delta E = 0.52$eV suggests that the new band is in fact the <100> and not the <111> minima. Also the energy separation of the (000) and <100> minima decreases with increasing temperature at a rate of 4×10^{-4}eV/^{o}K. Then in the high temperature region the electrons excited into the conduction band minima in the <100> directions will contribute appreciably to the conduction. The calculations described in the previous paragraph have been carried out for ratios of b_o/b_1 from 3 to 25 and it has been found that the energy separation of the two minima was quite insensitive to the value of the ratio of b_o/b_1. An average value of $\Delta E = 0.55 \pm .05$eV was obtained. Therefore, from the present calculations the energy separation of the (000) and <100> minima is $0.55 \pm .05$eV at ^{o}K. Since the temperature coefficient is

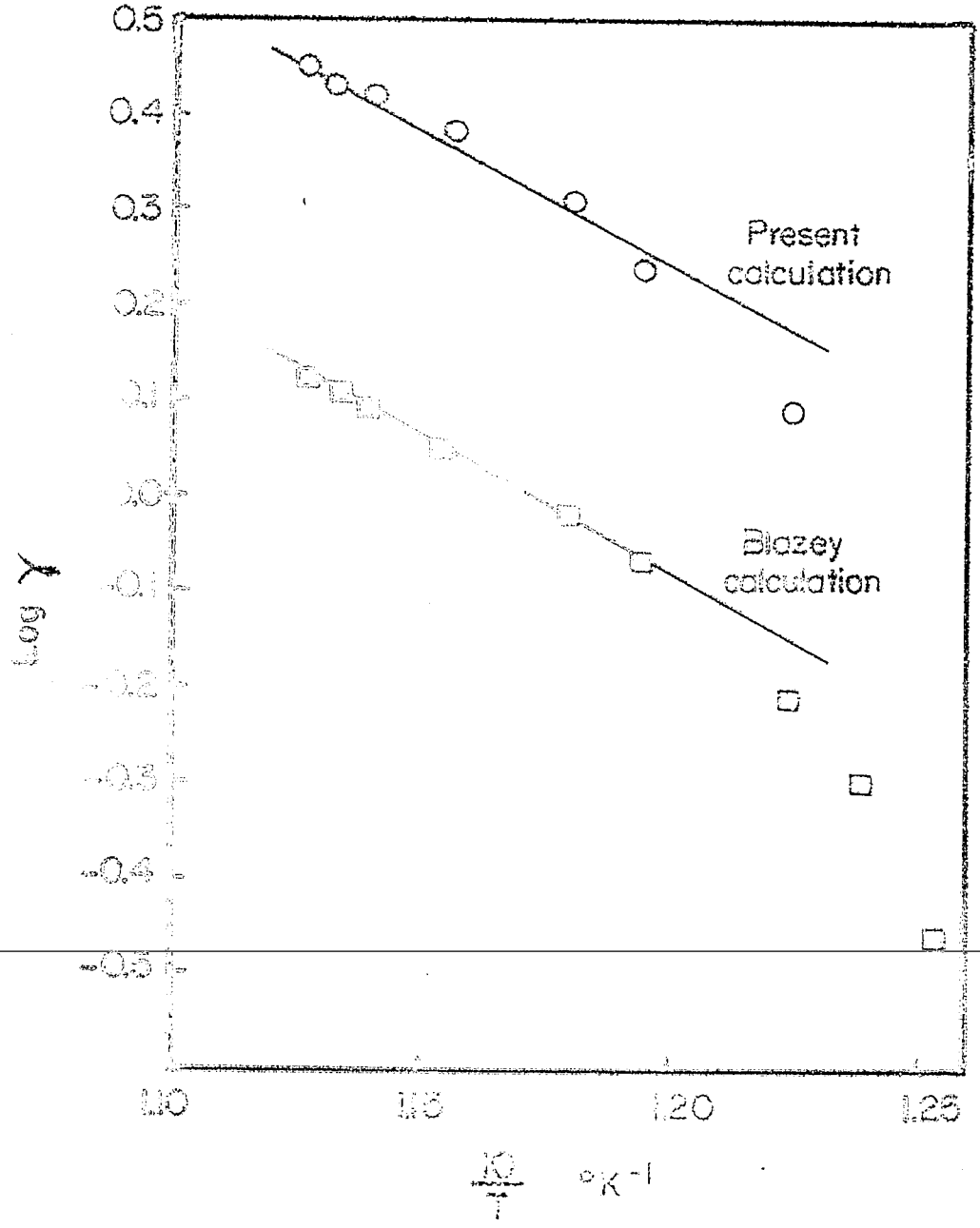

Fig. 16 Variation of $\log y = Ce^{\Delta E/kT}$ vs $10^3/T$ for GaSb.

$\sim 2 \times 10^{-4}$ eV/°K, ΔE at room temperature is 0.49eV. It has been estimated from pressure experiments (27) that ΔE at room temperature is approximately 0.4eV. The agreement between these two values for ΔE can be considered as excellent in view of the assumptions made in obtaining 0.49eV from the three carrier analysis and in view of the inaccuracy of the quoted 0.4eV estimated from pressure experiments. Finally, one can say that the low temperature electrical energy gap (0.82eV at 0°K) corresponds to electronic transitions from the valence band to the conduction minimum in the (000) direction and the slope of the $\log np/T^3$ vs. $1/T$ graph at high temperature (1.46eV at 0°K) is mainly determined by electrons in the conduction minima in the 100 directions. By adding the value of the direct band gap at 0°K (0.82eV) with the value of the energy separation of the (000) and <100> minima at 0°K(0.55eV) one obtains the height of the <100> minima above the valence band at 0°K(1.36eV). Of course one cannot expect good agreement with the slope of the $\log np/T^3$ graph at high temperature (1.46ev) because this value was obtained from a two carrier analysis of the Hall effect measurements. Now, it should be noticed that the slope of the $\ln RT^{3/2}$ vs. $1/T$ graph at high temperature for the 65-100 mol % CaSb alloys has no direct physical meaning and it cannot be called a high temperature electrical energy gap. A three carrier analysis (as it was done for CaSb) should be carried out on all of the alloys which show anomalous high temperature behaviour. However as yet insufficient data is available on the alloys to allow such an analysis to be carried out.

From the above results one sees that the high temperature slope for the 65-100 mol % CaSb alloys can be attributed to electronic transitions from the valence band to the conduction band minima in the <100> directions. Then, the experimental results for the band

structure of the InSb-GaSb alloy system can be explain by the following model. For compositions between 0 and 65 mol % GaSb the addition of GaSb to InSb progressively changes the value of the energy gap without causing any change in the general from of the band structure. The band form of the InSb and GaSb with the conduction band minimum at (000) in k-space is retained by the alloys in this composition range. The same thing applies for compositions between 65 and 100 mol % GaSb if one considers the optical energy gaps which represent low temperature conditions. For the composition range 65-100 mol % GaSb the so-called "high temperature electrical energy gap" is caused by a band change at high temperatures. The decrease of this so-called "high temperature electrical energy gap" with InSb concentration is due to the decrease in the effect of the <100> conduction band minima as the InSb concentration of the alloys increases.

It was seen in section 3.4 that the Hall mobility decreases as the GaSb concentration increases. This behaviour is due to scattering by the random arrangement of atoms on the lattice sites. Two other factors influence the value of the mobility for the alloys, (i) the increase in effective mass as the GaSb content of the alloys is increased, (ii) the interband scattering which can be expected to occur with GaSb and alloys close to this composition. From the relation $\mu =$ content T^{-x}, the temperature mobility exponent x was determined at high temperature and it was seen in the previous section that the high values of x decreases as the GaSb concentration decreases (in the range studied). At high temperature lattice scattering should predominate but the scattering processes are complicated by the effects discussed previously, and this is about what can be said about these high values of x at this stage. These high values of x were also obtained by Woolley and Elliott (9) in their investigation of the p-type alloys.

Chapter 4

The InAs - In_2SnTe Cross-Substitutional Alloy System.

4.1. Introduction.

It was seen in section 1.4 of chapter 1 that InAs and In_2SnTe are derived, by the process of cross-substitution, from Ge and InAs respectively. In practise In_2SnTe is unstable and so it is not formed. However, it is possible to replace only some of the As atoms by combination of Sn and Te and the resulting materials can be considered as alloys between InAs and the derived ternary compound In_2SnTe. It can be shown (19), from thermodynamic considerations, that InAs - In_2SnTe alloys are non-stoichiometric; some solution of Sn in the In lattice occurs and leaves excess Te on the As lattice. Both the Sn and the resulting excess Te act as donors and give n-type material of high carrier concentration. It was also seen in section 1.4 that by excessive doping of InSb and InAs the height of the second lowest conduction band minimum above the valence band may be determined. The InAs - In_2SnTe alloy system was investigated by determining the range of solid solution in InAs and by measuring the Hall coefficient and optical energy gap, as a function of composition, at room temperature. In the next sections of this chapter, these investigations will be described and the results discussed by means of the model proposed by Woodley (20).

4.2. Preparation of the InAs - In_2SnTe alloys.

The preparation of the InAs - In_2SnTe alloys will be briefly outlined because the same technique was used to prepare the InSb-GaSb

alloys but, the InAs - In_2SnTe alloys did not undergo the directional freezing.

The InAs used to prepare the alloys was obtained from the Consolidated Mining and Smelting Corporation of Canada Limited. It was supplied in the form of a polycrystalline ingot and was n-type with 2.2×10^{16} carriers cm^{-3} and a resistivity of 0.012 ohm-cm. at room temperature.

The In_2SnTe was made in a 5 gram ingot from 99.999% purity In, Sn and Te. The stoichiometric quantities of the elements were melted together in a sealed, evacuated quartz tube and quenched in air.

Similarly, the InAs - In_2SnTe alloys were prepared with the appropriate quantities of the constituent compounds.

4.3. Determination of the range of solid solution in the InAs-In_2SnTe alloy system.

Alloys containing 1, 2, 5, 10, 20 and 40 mol % In_2SnTe were made as outlined in the previous section. These air quenched alloys were powdered and X-rayed with a 11.483 cm Debijer Scherrer powder camera using CuKα radiation. The X-ray photographs showed that all the alloys had a zinc-blende structure. The alloys containing 1 and 2 mol % In_2SnTe were single phase and all the others showed faint traces of a second phase. The X-ray lines were reasonably sharp in all the photographs and the lattice parameter was determined for each alloy. The powdered specimens were compressed and annealed in vacuum for 4 weeks at 400°C. The specimens were X-rayed again and the results were the same as those prior to the

annealing. A graph of the variation of the lattice parameter as a function of composition is shown in Fig. 17. From this graph it can be seen that the equilibrium range of solid solution at 400°C is 3 mol % In_2SnTe.

4.4. Electrical measurements.

It was seen that alloys containing small amounts of ternary compound are the important ones for electrical and optical measurements. Alloys containing 0.1, 0.2, 0.3, 0.5 and 1 and 2 mol % In_2SnTe were prepared as outlined in section 4.2 and annealed in vacuum for 10 days at 400°C to ensure complete equilibrium. Specimens for Hall effect measurements were cut from these 4 gram ingots and etched in Wolsky to clean the surfaces. Etchant Wolsky consists of 1 part concentrated nitric acid, 7 parts concentrated hydrochloric acid and 8 parts glacial acetic acid.

The Hall coefficient, at room temperature, was determined by the same technique as the one used for the InSb-GaSb alloys. The values of the Hall coefficient showed that all alloys were n-type, and assuming that $R_{HS} = \frac{1}{ne}$ for these materials, highly degenerate values of n were obtained. A graph of the variation of log n against composition is shown in Fig. 17. It is seen that n rises sharply and becomes constant at an approximate value of $4.4 \cdot 10^{19}$ carriers cm^{-3}. It has been found by Woolley and Williams (20) that the electrical results for the cross-substitutional alloys of InSb were independent of temperature. Hence the room temperature results can be taken as characteristic of these highly degenerate materials.

4.5. Optical measurements.

4.5.1. Preparation of specimens for infra-red transmission measurements.

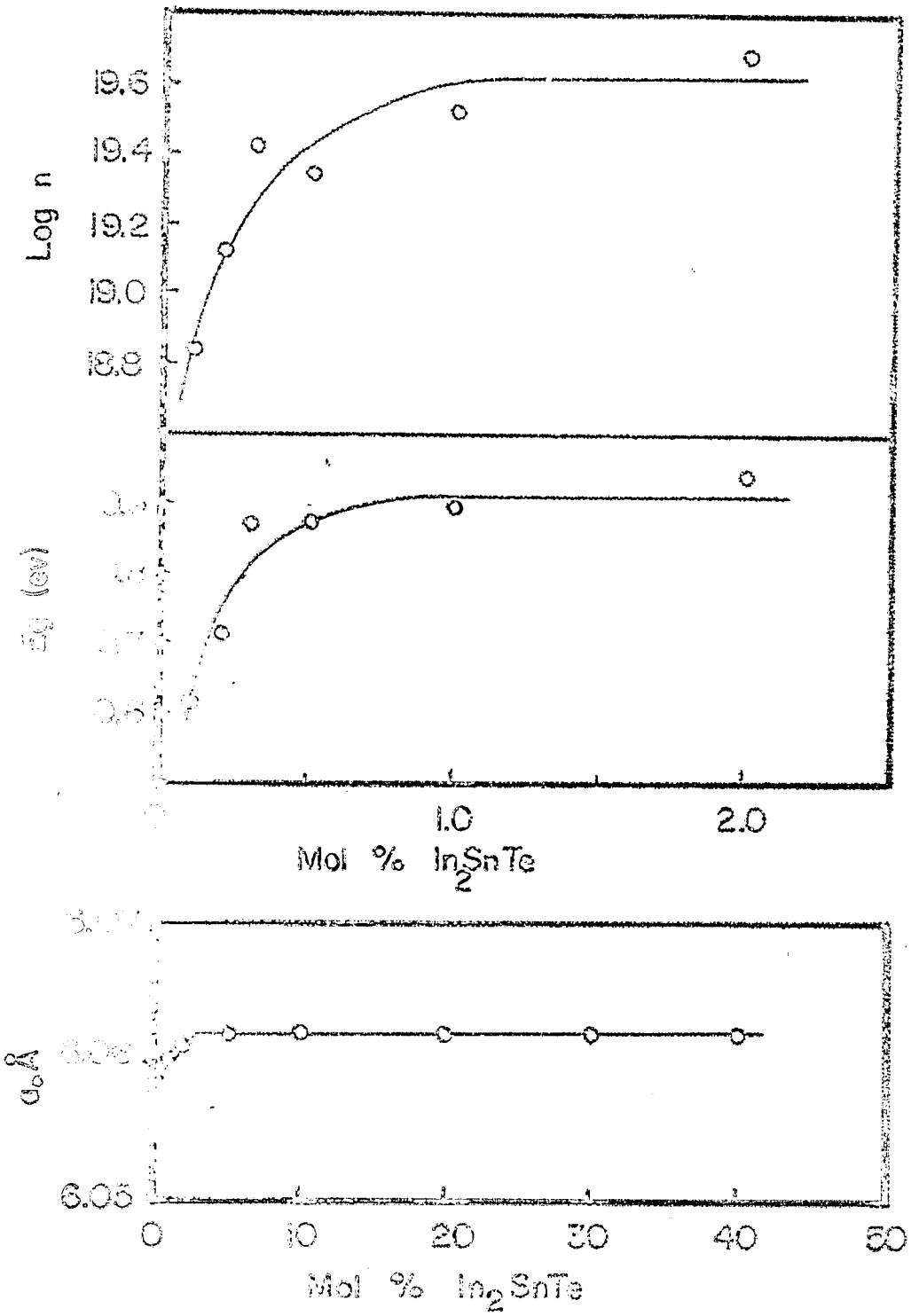

Fig. 17 Variation of electron density n, optical energy gap Eg, and lattice parameter a_o with composition for InAs-In_2SnTe alloy system.

In order to measure the optical energy gap as a function of composition thin slices, about 1 mm thickness, were cut from the same ingots which were used to obtain Hall effect specimens. The slices were then ground and polished in the following way. A slice was stuck, with "glyptal cement", on a small flat circular bass disc which was screwed into a steel rod. The rod was fitted into a bearing which was held fixed over a polishing wheel so that while the wheel was rotating the specimen was spinning. Two rotating wheels were used to carry out the polishing, one was covered with a soft emery paper and the other with a Buehler micro-cloth. First, the slice was ground on the emery paper until it was approximately 300 microns thickness. The rough surface remaining after the grinding was removed by polishing the specimen on the micro-cloth which was continually covered with a thin layer of a mixture of water and 5 micron alumina powder. The specimen was taken off the disc by dissolving the glue with acetone and it was turned over. The other side was polished until the slice was approximately 120 microns thickness. Slices of this thickness were suitable for infra-red transmission measurements.

4.5.2. Method of measurements.

A schematic diagram of the optical apparatus used with a single beam, double pass, Perkin-Elmer infra-red spectrometer is shown in Fig. 18. The source of radiation was a Nearst filament and a NaCl prism provided the necessary dispersion. The radiation coming from the source was chopped at 13 cycles per second, detected by a thermocouple, amplified, and recorded by a Brown recording potentiometer. The spectrometer was calibrated by means of didymium glass (0.54-2.42 μ), polystorene (2.42-7.47 μ) and CO_2 in the atmosphere (4.225 μ). The calibration curve is shown in Fig. 19.

A sample under investigation was mounted over a slot in a brass disc. The disc fitted into a sliding mechanism so that the

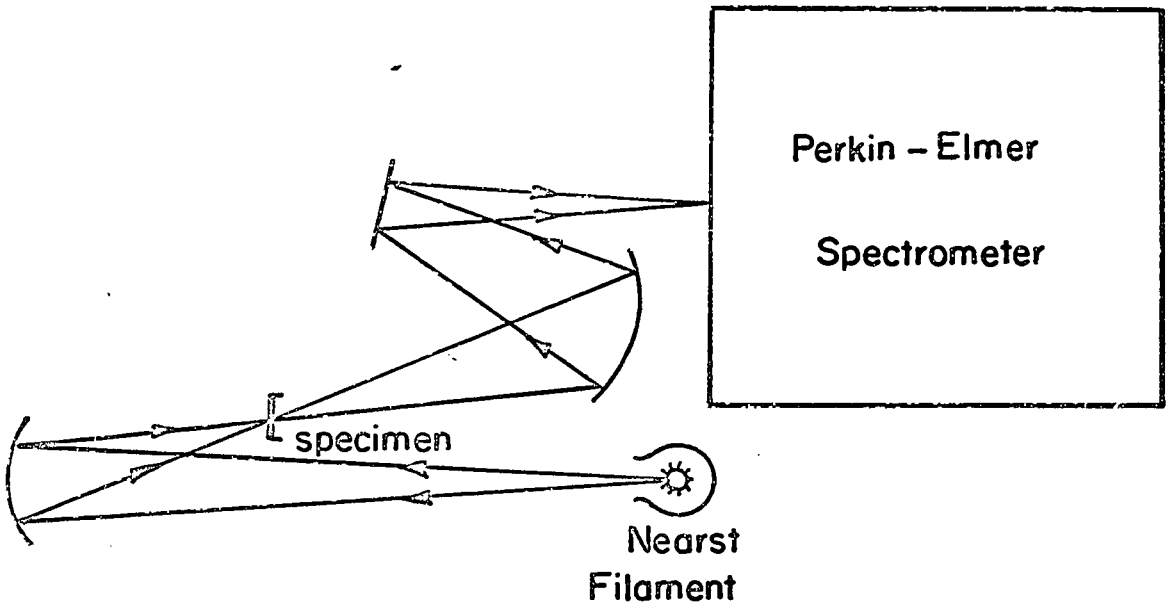

Fig. 18 Schematic diagram of optical apparatus.

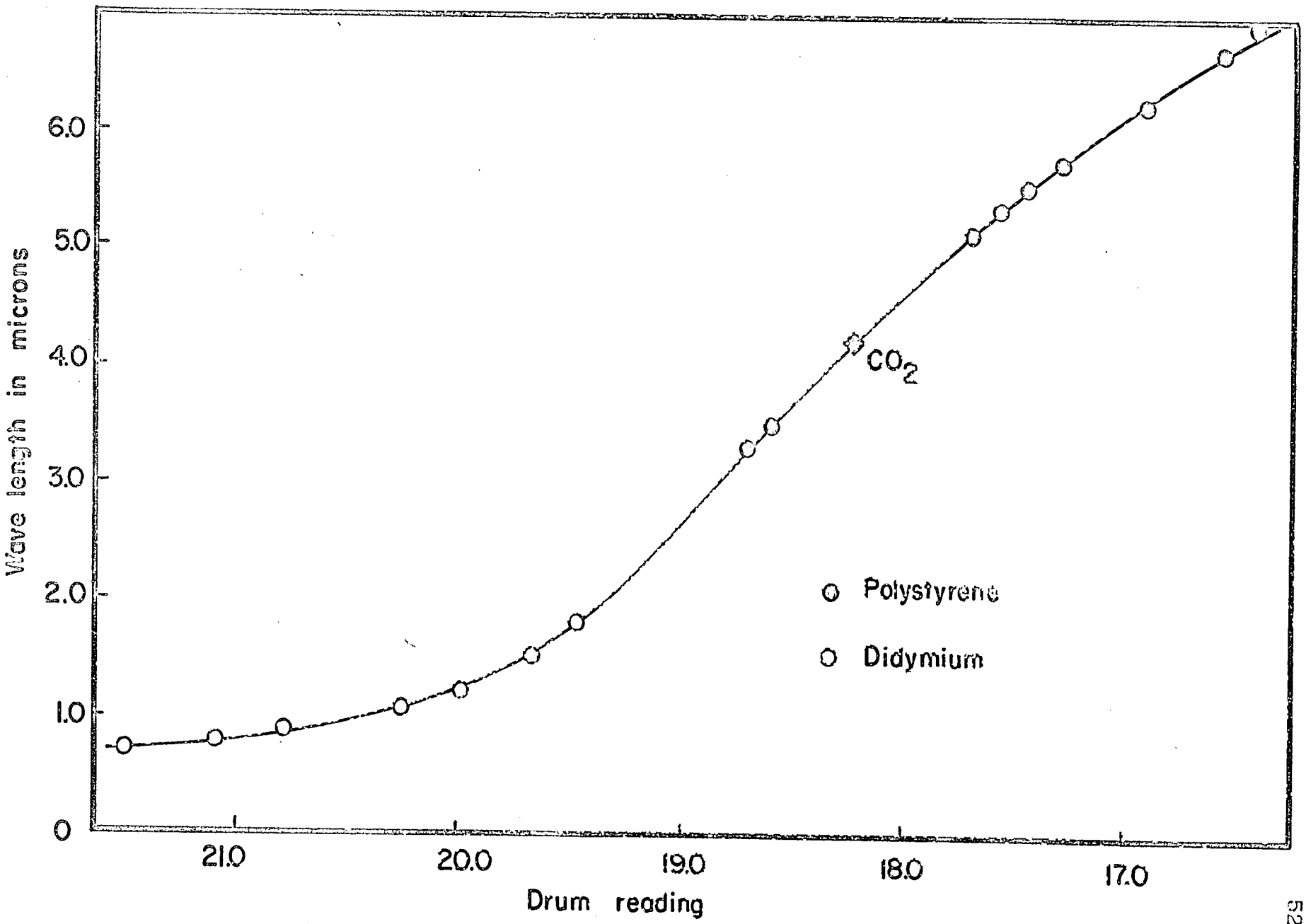

Fig. 19 Calibration of Perkin-Elmer infra-red spectrometer, NaCl prism

specimen could easily be inserted into the radiation beam, as shown in Fig. 18. The intensity I_o of the incident radiation, with the specimen out of the beam, and the intensity I of the transmitted radiation, with the specimen in the beam, were read directly from the potentiometer as a function of the drum reading or wavelength. The infra-red absorption spectrum of a typical specimen is shown in Fig. 20.

4.5.3. Results.

The infra-red absorption curve shown in Fig. 20 is seen to exhibit typical semiconductor features: an opaque region to the shortest wavelengths which results from interband absorption, a relatively sharp absorption edge, and a partially transparent region beyond the edge in which free-carrier absorption is predominant. The gradual decrease in transmission observed on the long wavelength side results from the usual increase in free-carrier absorption with increasing wavelength.

The optical energy gap was determined from the infra-red absorption curves by the method described in section 1.5 of chapter 1. A graph of the variation of the optical energy gap against composition is shown in Fig. 17. It is seen that the absorption edge shifts to shorter wavelengths with increasing In_2SnTe concentration, reaches a maximum of 0.99 ev at 1 mol % $InSnTe$ and remains constant at that value for larger In_2SnTe content.

4.6. Discussion of the results.

It was seen that the large density of electrons in the InAs-In_2SnTe alloys was due to the non-stoichiometry of the alloys. As suggested by Woolley (30), the maximum value of 4.4×10^{19} carriers

specimen could easily be inserted into the radiation beam, as shown in Fig. 18. The intensity I_o of the incident radiation, with the specimen out of the beam, and the intensity I of the transmitted radiation, with the specimen in the beam, were read directly from the potentiometer as a function of the drum reading or wavelength. The infra-red absorption spectrum of a typical specimen is shown in Fig. 20.

4.5.3. Results.

The infra-red absorption curve shown in Fig. 20 is seen to exhibit typical semiconductor features: an opaque region to the shortest wavelengths which results from interband absorption, a relatively sharp absorption edge, and a partially transparent region beyond the edge in which free-carrier absorption is predominant. The gradual decrease in transmission observed on the long wavelength side results from the usual increase in free-carrier absorption with increasing wavelength.

The optical energy gap was determined from the infra-red absorption curves by the method described in section 1.5 of chapter 1. A graph of the variation of the optical energy gap against composition is shown in Fig. 17. It is seen that the absorption edge shifts to shorter wavelengths with increasing In_2SnTe concentration, reaches a maximum of 0.90 ev at 1 mol % InSnTe and remains constant at that value for larger In_2SnTe content.

4.6. Discussion of the results.

It was seen that the large density of electrons in the InAs-In_2SnTe alloys was due to the non-stoichiometry of the alloys. As suggested by Woolley (39), the maximum value of 4.4×10^{19} carriers

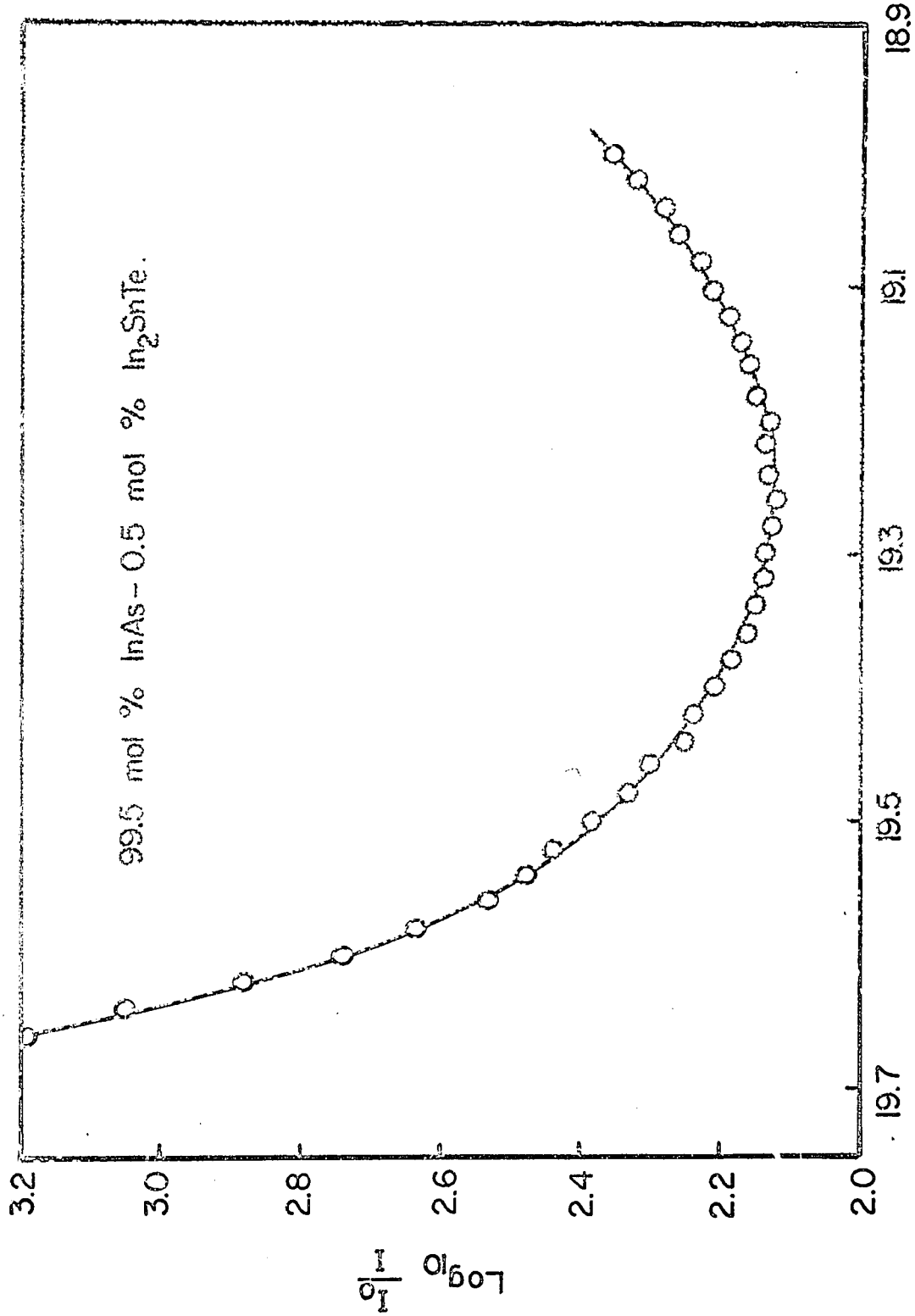

Fig. 20 Infra-red transmission spectrum of an InAs – In_2SnTe alloy.

cm^{-3} is determined by the band structure of InAs. Many more Te atoms than those giving this maximum value act as donors in the alloys, but the extra electrons enter other much broader conduction band minima and are not observed by Hall effect measurements because of a much larger effective mass than electrons in the (000) minimum. The fast increase of the optical energy gap at low In_2SnTe concentrations is due to the Burstein effect. The absorption edge shifts to shorter wavelengths with increasing electron concentration as observed in InSb (28) and InAs (29). These shifts are attributed to the low density of states in the conduction bands of these compounds. When the free electron concentration is sufficient to fill an appreciable fraction of the lower states in the conduction band, photons of higher energy are required to promote electrons from the valence band to higher unoccupied states. Therefore the shift of absorption edge may be taken as evidence for a low electron effective mass. (For InAs, m_n = 0.03 m). There is no further increase in the optical energy gap beyond 1% In_2SnTe because of the much higher density of states in the other minima, presumably the <111> minima. Thus, the observed maximum value of n(≈ 4×10^{19} carriers cm^{-3}) is the density of electrons required to fill the (000) minimum up to the lowest level of the <111> minima and the observed maximum value of the optical energy gap (0.90 ev) gives the height of the <111> minima above the valence band maximum. The InAs-In_2GeSe and InAs-In_2GeTe alloys systems were investigated by Dr. E.W. Williams (30) and the results were identical to those of the InAs-In_2SnTe alloys system. This indicates that the observed maximum values of n and E_g are independent of the source of electrons provided the band structure is not affected by the addition of the donor atoms.

Appendix

It is intended to reproduce the main parts of the three carrier analysis of GaSb carried out by Blaney (24). As indicated in the third chapter of this thesis, the analysis has been corrected and extended in order to explain the low and high temperature electrical energy gap in GaSb.

Measurement of the Hall effect as a function of temperature for GaSb showed that at low temperature it was p-type with 10^{17} extrinsic carriers per cc. As the temperature was raised intrinsic behaviour became dominant. It will be assumed that electrons were being excited principally into the conduction band minimum at k = 000 at these lower temperatures. According to Sagar's conduction band model of GaSb (25) electrons will also be excited to the heavy mass conduction band minima in the <111> directions as the temperature is increased further. Thus the intrinsic region may be considered as being split into two parts. One of these, the low temperature section, is when the conduction is carried out principally by the holes in the valence band and electrons in the conduction band minimum at k = 000 only. At higher temperature the electrons excited into the conduction band minima in the <111> directions, as well as the other two types of carriers, will contribute appreciably to the conduction processes.

The intrinsic number of carriers, n_o, in the conduction band minimum at k = 000 is given by the equation:

$$n_o p = \left(\frac{2\pi kT}{h^2}\right)^3 (m_n^o m_p)^{3/2} e^{\frac{-E_o + \beta_o T}{kT}} \qquad (1)$$

where m_n^o is the electron effective mass at k = 000, m_p the hole

effective mass at k = 000, E_o the direct band gap at 0°K, β_o the temperature coefficient of the direct band gap, and p the number of holes in the valence band. This equation assumes the existence of parabolic bands and spherical energy surfaces in k-space. The intrinsic carrier concentration, n_1, in the conduction band minima in the <111> directions is given by the equation:

$$n_1 p = 4\left(\frac{2\pi kT}{h^2}\right)^3 (m_n^l m_p)^{3/2} e^{-\frac{E_1 + \beta_1 T}{kT}} \qquad (2)$$

where m_n^l is the electron effective mass in the <111> directions, E_1 the indirect band gap at 0°K, and β_1 the temperature coefficient of the indirect band gap. Dividing equation (1) and (2) give the ratio of the number of carriers in the two conduction band minima

$$\frac{n_1}{n_o} = C\, e^{\Delta E/kT} \qquad (3)$$

where ΔE is the energy separation of the two conduction band minima and C a constant involving the carrier effective masses and the temperature coefficient of the band gaps, both parameters are assumed to be temperature independent.

In the low temperature intrinsic region where there are only two contributing carriers to the Hall effect, the Hall coefficient is given by:

$$R_H = \frac{n_o b_o^2 - p}{(n_o b_o + p)^2} \qquad (4)$$

where b_o is the mobility ratio of the electrons and holes at k = 000. For a p-type semiconductor with p_e extrinsic carriers per cc.

$$p = n_o + p_e \qquad (5)$$

From equations (4) and (5) the electron concentration at k = 000 is given by

$$n_o = \frac{(b_o - 1)}{2e(b_o + 1)R} - \frac{p_o}{b_o + 1} \pm \frac{1}{(b_o+1)}\left[\frac{(b_o-1)^2}{4R^2e^2} - \frac{p_o b_o}{Re}\right]^{\frac{1}{2}} \quad (6)$$

If it is assumed that at low temperature the intrinsic contribution is negligible so that

$$\rho_{ext} = \frac{1}{p_e e} \quad (7)$$

then it may be shown that

$$\frac{R_{max}}{R_{ext}} = \frac{(b_o-1)^2}{4b_o} \quad (8)$$

where R_{max} is the maximum value attained by the Hall coefficient above the Hall inversion temperature. Thus from the values of the Hall coefficient as a function of temperature the mobility ratio of the electrons in the conduction band minimum at k = 000 to the holes in the valence band may be evaluated. From equation (5) and (6) the number of holes in the valence band and the number of intrinsic electrons in the conduction band at k = 000 may be calculated. These values were substituted in the following equation:

$$\log_{10}\frac{a_o p}{T^3} = \log_{10} A + \frac{3}{2}\log_{10}(m_a^o m_p) - \frac{E_o}{2.303kT} + \frac{\varphi_o}{2.303k} \quad (9)$$

The gradient of the graph of $\log_{10} a_o p/T^3$ against $1/T$ gives the energy gap E_o. The value obtained from the low temperature intrinsic region was in good agreement with values obtained by other experiments for the direct band gap at k = 000 in GaSb.

Above the transition temperature, T_c, not only are the electrons in the conduction band minimum at k = 000 contributing to the conduction processes, but also those in the minima in the <111> directions start contributing noticeably, so the Hall coefficient becomes:

$$R_e = \frac{n_o b_o^2 + n_1 b_1^2 - p}{(n_o b_o + n_1 b_1 + p)^2} \tag{10}$$

where b_1 is the mobility ratio of the electrons in the <111> minima and the holes in the valence band. The number of holes is now given by:

$$p = n_e + n_1 + p_e \tag{11}$$

therefore

$$R_e = \frac{n_o(b_o^2-1) + n_1(b_1^2-1)-p_e}{\left[n_o(b_o+1)+n_1(b_1+1)+p_e\right]^2} \tag{12}$$

Substituting for $Ce^{-E/kT}$ the result is

$$Ce^{\Delta E/kT} = \frac{(b_1-1)-2Ren_o(b_o+1)-2Rep_e}{2Ren_o(b_1+1)} \pm \frac{\left[(b_1-1)^2+4Ren_o(b_o-b_1)(b_o+1)-4Rep_e b_1\right]^{\frac{1}{2}}}{2Ren_o(b_1+1)} \tag{13}$$

It will be assumed that $n_o p/T^3$ behaves in the same way at temperatures above T_c as it does below this temperature. Thus since it is assumed that below T_c $n \approx n_o$, values of n_o above T_c can be obtained by extrapolation of the $\log_{10} np/T^3$ against $1/T$ graph to temperature above T_c. The relation used here between b_1 and b_o was given by Sagar (25), and is $b_o = 6b_1$. Therefore, from the measured values of the Hall coefficient the value of $C e^{-\Delta E/kT}$ may be calculated as a function of

temperature. The gradient of a graph of log $C\, e^{\Delta E/kT}$ against $\frac{1}{T}$ gives the energy separation ΔE of the two conduction band minima.

From the measurements of the Hall coefficients as a function of temperature, graph of log np/T^3 against $10^3/T$ and log $C\, e^{\Delta E/kT}$ against $10^3/T$ were drawn and are shown in Fig. 15 and Fig. 16 respectively.

The graph of log np/T^3 against $10^3/T$ has a discontinuity which breaks it into two parts of different slopes. The low temperature region gives an energy gap 0.81 eV which is in agreement with the values obtained by other workers. The high temperature region gives a value of 1.46 eV which is much larger than the value of 1.00 eV obtained by Gillett (9). The effect of the present result would be to remove the discontinuous variation of the high temperature energy gap in the region of 95 mol % GaSb shown in Fig. 5.

The graph of log $e^{\Delta E/kT}$ against $10^3/T$ is linear only at high temperature. The gradient of this graph gives the energy separation of the two conduction band minima as 0.32 eV at 0°K. The value quoted by Segar (25) is 0.08 eV at room temperature. The temperature coefficient of this band separation would therefore need to be -1.5×10^{-3} eV/$^\circ$K to make the two values compatible. This is in poor agreement with the value of -2×10^{-4} eV/$^\circ$K given by Segar. In fact more recent workers, Cardona and Piller (26) have given evidence that the separation of the band minima decreases as the temperature is decreased, at a rate of 10^{-4} eV/$^\circ$K. This latter value would predict an energy separation of about 0.05 eV at 0°K, a factor of ten smaller than the result of the above analysis.

References

1. L. Nordheim, Ann. Phys., Lpz. 9, 607, 641 (1931).
T. Muto, Sci. Pap. Inst. Phys. Chem. Res. (Tokyo) 34, 377 (1938).
R.H. Parmenter, Phys. Rev. 97, 587 (1955), 99, 1759 (1955),
104, 22 (1956).

2. J.C. Woolley, Preparation of III-V Compounds p. 3. (Editors,
R.K. Willardson and H.L. Reinhold), New-York (1962).

3. J.C. Woolley and B.A. Smith, Proc. Phys. Soc. 72, 214 (1958).

4. J.C. Woolley, B.A. Smith and D.G. Lees, Proc. Phys. Soc.
79, 1339 (1956).

5. J.C. Woolley, J.A. Evans and C.M. Gillett, Proc. Phys. Soc.
74, 244 (1959).

6. J.C. Woolley, J.A. Evans, Proc. Phys. Soc. 78, 354 (1961).

7. J.C. Woolley, K.W. Blazey, J. Phys. Chem. Solids 25, 713 (1964).

8. J.C. Phillips, Phys. Rev. 125, 1931 (1962).

9. J.C. Woolley and C.M. Gillett, J. Phys. Chem. Solids 17, 34 (1960).

10. R.A. Smith, Semiconductors, Cambridge University Press,
London (1961).

11. J.C. Woolley and B. Ray, J. Phys. Chem. Solids 15, 27 (1960).

12. A.I. Aptekar and B. Finkelshtein Zh. eksp. theor. fiz. 21, 900 (1951).

13. J.C. Woolley and D.G. Lees, J. Less Common Metals 1, 192 (1959).

14. J.C. Woolley and A.C. Briggs, J. Phys. Chem. Solids 25,
895 (1964).

15. B. Abeles, Phys. Rev. 131, 1906 (1963).

16. C.H.L. Goodman, J. Phys. Chem. Solids 6, 305 (1958)
J.E. Wernick and R. Wolfe, Electronics 33, (Feb. 12, 1960).

17. D.B. Casson, P.J. Holmes, I.C. Jennings, B.R. Marathe, and J.E. Parrot, J. Phys. Chem. Solids 23, 1291 (1962).
A.J. Strauss and A.J. Rosenberg, Ibid. 17, 278 (1961).
W.G. Spitzer, J.M. Warnick, and R. Wolfe, Solid State Electronics 2, 96 (1961).

18. N.A. Goryunova and V.D. Prochukhan, Soviet Physics Solid State 2, 161 (1960).

19. D.B. Casson, I.C. Jennings, J.E. Parrott and A.W. Penn, Proc. Int. Conf. on Physics of Semiconductors, Exeter, p. 681 (1962).

20. J.C. Woolley and E.W. Williams, J. Electrochem. Soc. 111, 210 (1964).

21. J.E. Parrott, J. Phys. Chem. Solids 23, 1437 (1962).

22. J.C. Woolley, C.M. Gillett and J.A. Evans, J. Phys. Chem. Solids 16, 138 (1960).
J.C. Woolley and P.M. Keating, Proc. Phys. Soc. 78, 504 (1961).
J.C. Woolley, B.R. Pamplin and J.A. Evans, J. Phys. Chem. Solids 19, 147 (1961).

23. D. Mier and P.J. Etter, J. Phys. Chem. Solids 25, 451 (1964).
D.F. Detwiler, Phys. Rev. 97, 1575 (1955).
H. Welker, Physica 20, 893 (1954).

24. K. Blazey, Ph.D. Thesis, Nottingham University, England (1964).

25. A. Sagar, Phys. Rev. 117, 93 (1960).

26. M. Cardona, J. Phys. Chem. Solids 17, 336 (1961).
M. Piller, J. Phys. Chem. Solids 24, 425 (1963).

27. A. Segar and R. C. Miller, J. Appl. Phys. 32, 2373 (1961).
H. Ehrenreich, J. Appl. Phys. 32, 2155 (1961).

28. E. Burstein, Phys. Rev. 93, 632 (1954).

29. F. Stern and R. M. Talley, Phys. Rev. 100, 1638 (1955).

30. E. W. Williams, Ph. D. Thesis, Nottingham University, England (1964).

Discussion of errors.

The InSb-GaSb semiconducting alloys.

It must be remember that certain errors have been discussed previously. One type of errors was due to the formulae used to determine the electrical energy gaps. This has been discussed in section 1.5 of chapter I and in section 3.4 of chapter 3. The precautions taken to eliminate or reduce the experimental errors were stated in the proper sections. The purpose of this section is to give a value of the error, in the energy gaps, due to the scattering of the experimental points on the graphs of $\ln R_H^3$ vs. 1/T. The scattering in the value of each slope is approximately 5%, this the exprimental error in the energy gaps. This error is greater than that found by using the standard formulae for calculating errors.

The InAs-In_2SnTe semiconducting alloys.

In the case of these alloys, the scattering from a smooth curve of the electron concentrations and optical energy gaps as a function of composition (Fig.17) is greater than the experimental error. It must be pointed out that this does not invalidate the conclusions of section 4.6 of chapter 4. Also it was stated in that section that the final results agree well with those of Williams(30) who has investigated the InAs-In_2GeSe and InAs-In_2GeTe systems. The scattering is believed to be due to the following factors: (1) a non-complete diffusion of impurities (small concentration of In_2SnTe), the ingots were kept in the liquid state for approximately 30 minutes, and (2) some of the impurities may have vaporized and, on cooling, condensed on the walls, or diffused into the quartz. A few measurements were reapeated on the same specimens and the results were reproducible within a few per cents.

VITA

NAME	Reynald Gagnon
BORN	Rivière Ouelle, Québec 1938
EDUCATED	
Primary	Ecole No. 1, Rivière-Ouelle, Québec, 1944-1955
Secondary	Académie D.L.S., Trois-Rivières, Québec, 1955-57
University	Ottawa, Ontario, 1957-64
Course	Physics
Degree	B.Sc. (Honours) 1963
APPOINTMENT	Assistant in the Department of Physics, Toronto University, Ontario 1964-